Properties of Vacuum and Gas Diodes

H. J. OSKAM, Chief Investigator
Report Prepared by
H. J. OSKAM
and
C. BRUCE JOHNSON

PLASMA PHYSICS RESEARCH LABORATORY
UNIVERSITY OF MINNESOTA
INSTITUTE OF TECHNOLOGY

Contract No. AF 19(604)-8072

Scientific Report No. 1

March 1963

Prepared for

ELECTRONICS RESEARCH DIRECTORATE
AIR FORCE CAMBRIDGE RESEARCH LABORATORIES
OFFICE OF AEROSPACE RESEARCH
UNITED STATES AIR FORCE
BEDFORD, MASSACHUSETTS

Requests for additional copies by Agencies of the Department of Defense, their contractors, and other Government agencies should be directed to the

ARMED SERVICES TECHNICAL INFORMATION AGENCY
ARLINGTON HALL STATION
ARLINGTON 12, VIRGINIA

Department of Defense contractors must be established for ASTIA services or have their "need-to-know" certified by the cognizant military agency of their project or contract.

All other persons and organizations should apply to the:

U. S. DEPARTMENT OF COMMERCE
OFFICE OF TECHNICAL SERVICES
WASHINGTON 25, D. C.

Foreword

This technical report was prepared by Dr. Hendrik J. Oskam and C. Bruce Johnson of the Electrical Engineering Department, University of Minnesota under Air Force Contract AF 19(604)-8072.

This report covers the part of the research effort as carried out by C. Bruce Johnson during the period February 1961 to February 1963.

The work was administered under the direction of the Electronics Systems Division, Air Force Systems Command, Laurence G. Hanscom Field, with Dr. Norman Rosenberg as the task engineer.

Abstract

This technical report is concerned with the properties of vacuum and gas diodes. The equations describing the properties of these two types of diodes are compared for the situation in which the diode current is space-charge limited.

The screen anode of an auxiliary discharge is used as the cathode of the gas diode and the properties of this type of cathode were studied and the experimental results are reported.

Table of Contents

Table of Contents (continued)

List of Illustrations

List of Illustrations (continued)

Chapter 1

Introduction

The parameters describing the motion of charged particles in vacuum under the influence of externally applied force fields have been of interest for several decades. As a matter of fact, the operating characteristics of the various types of vacuum tubes used in a large number of electronic devices are based on the laws governing the motion of charged particles in vacuum.

During the last decade the motion of charged particles in a gaseous environment has witnessed a renewed interest. This is due mainly to the realization that the study of the properties of gaseous plasmas could lead to a better understanding of the physics of ionosphere and interstellar phenomena, etc. Moreover, these studies might lead to applications in the field of plasma and ion propulsion techniques, the generation of power by means of the nuclear fusion process, etc.

Another research effort, which deserves interest, is that related to the direct conversion of thermionic energy into electric energy. Various energy conversion efforts have been made. However, most of these efforts concern the fabrication of practical devices, without the detailed knowledge of the basic physical operating principles involved.[1,2]

The thermionic energy converter, using a neutral or partly ionized gas as a conductor, consists of a hot cathode (the thermionic energy) and a collector (anode). The difference between the work functions of the two electrodes supplies the potential

difference necessary to induce the electrons emitted by the hot cathode to reach the anode. The product of the tube current and the external voltage represents the electrical power delivered by the thermionic energy converter.

During the early development of the thermionic converter the volume between the two electrodes did not contain gas atoms (vacuum converter). However, the electrode separations required to eliminate the influence of the negative space-charge barrier in front of the hot cathode were found to be impractically small. Therefore, cesium gas was admitted so that, due to the surface ionization process of cesium atoms at the hot cathode surface, part of the space-charge barrier could be eliminated while keeping the electrode separated within practical limits. However, due to the presence of the cesium gas atoms, the motion of the charged particle within the converter diode could not be considered to be the same as that in vacuum.

Rather recently it was found that the thermionic energy converter operated with the highest converter efficiency when a gaseous plasma was present within the converter. The ions produced inside the plasma neutralized the negative space-charge barrier completely so that the diode current can be made equal to the hot cathode saturation current.

Although the cesium plasma converter seems promising, it shows a large number of technological problems. Recently, various investigators have directed their interest towards the rare gas converter, in which the positive ions needed for the neutralization

of the negative space-charge barrier are produced by means of an auxiliary discharge. It is hoped that by using this technique the electrical power needed for maintaining the auxiliary discharge is considerably smaller than the power delivered by the thermionic energy converter.

From this very brief historical survey of the direction in which a solution is being sought for the efficient conversion of thermionic energy into electrical energy, it is obvious that a study of the laws governing the motion of charged particles in a neutral or ionized gas under the influence of an externally applied electric field is of importance. Since most of the efforts have been devoted to the development of practical converters, the experimental parameters have not in general been varied. Consequently, most of the basic information required for understanding their operating characteristics is not available.

In the next chapters, studies concerning the motion of charged particles in a gas diode will be reported. The laws relating to the vacuum diode as well as to the gas diode are presented in Chapter 2. This facilitates the investigation of the influence of the presence of the gas particles on the properties of a diode. The main emphasis is placed on the situation in which the tube current is space-charge limited. A brief summary of previous studies is given in Chapter 3.

The equipment developed and constructed for the experimental study of the properties of a gas diode is described in Chapter 4. In order to avoid the difficulties inherent to the use of a hot

cathode, which induces a large temperature gradient and thus a particle density gradient inside the tube so that comparison with theory is difficult, a special type of emitter was used. Emitters of this general type have been reported in the literature.[3-9] The emitter is, in reality, a fine mesh screen which serves as the anode of an auxiliary gaseous discharge. Part of the charged particles reaching their screen anode pass through it and enter the gas diode region. The parameters of the auxiliary discharge determine the number of charged particles entering the gas diode as well as their velocity distribution function and thus the "temperature" of the emitter.

During the early stages of these studies, it was found necessary first to investigate the influence of the discharge parameters on the properties of the screen emitter. The relevant relationships are discussed in Chapter 5 and the experimental data are presented in Chapter 6.

The use of a specially developed collector combined with the screen emitter made it possible to study the velocity distribution function of the electrons in the discharge region adjacent to the screen anode. The variation of the electron velocity distribution in these regions could be determined by placing the screen anode in the various discharge regions.

The results are summarized in the last chapter, where the future plans are also mentioned.

References

1. J. Kaye and J. A. Welsh, "Direct Conversion of Heat to Electricity," John Wiley and Sons, Inc., New York, 1960.
2. S. N. Levin, "Selected Papers on New Techniques for Energy Conversion," Dover Publications, Inc., New York, 1961.
3. J. Nienhold, German Patents No. 319,806; 331,029; 345,921, 345,276, 1916 through 1919.
4. A. Hund, Electronics 6, 6 (1933).
5. F. Schroter, Electronics 8, 131 (1935).
6. H. C. Boumeister and M. J. Druyvesteyn, Philips Tech. Rev. 1, 367 (1936).
7. J. D. LeVan and P. T. Weeks, Proc. I.R.E. 24, 180 (1936).
8. J. M. Lafferty, I.R.E. Trans. on Electron Devices ED-5, 143-147 (1958).
9. J. M. Anderson and L. A. Harris, J. Appl. Phys. 31, 1463-1468 (1960).

Chapter 2

Theory of Vacuum and Gas Diodes

2.1 Introduction

In the first part of this chapter the theory of the vacuum diode will be discussed. The main reason of presenting the various formulae relating to this type of diode is to have the possibility of comparing these formulae with those found for the gas diode in which the charged particles collide with neutral particles.

The theory of the vacuum diode has been discussed in the literature;[1-7] and the formulae obtained have been extensively confirmed by experiments. Therefore, only a summary of the results will be given, and the main emphasis will be directed toward understanding the physical principles.

In contrast to the large amount of studies relating to the vacuum diode, the number of investigations which could lead to a better knowledge of the physics of the gas diode is rather limited. Consequently, a detailed discussion of the theory concerning the motion of charged particles in a gas diode will be given in this chapter.

2.2 The Vacuum Diode

2.2.1 Introduction

The rigorous derivation of the current-voltage relation, valid for a vacuum diode, must take into account the energy distribution of the charged particles leaving the emitter. However, it is believed that more insight into the properties of the vacuum diode is obtained by first considering the situation in which the charged particles leave the emitter mono-energetically. After

this rather detailed discussion, the steps which are necessary for introducing the influence of the energy distribution are indicated.

The discussion will be confined mainly to the situation in which the diode current is space-charge limited. When the diode current is not space-charge limited the current is either completely cut-off or saturated. The last two situations give trivial voltage-current relationships.

2.2.2 The mono-energetic method

In this section the case in which charged particles with mass m and charge q leave the emitter with velocity v_o (normal to emitter) will be discussed. When the total emitted current density $J_o = \rho_o v_o$ (ρ_o space-charge density at the emitter) is collected the tube current is said to be saturated. This will occur when the kinetic energy of the charged particles contributing to the tube current is larger than zero at every point between emitter and collector.

The tube current is zero (cutoff condition) when none of the emitted particles reach the collector. When assuming an initial emission velocity this condition can exist only for a sufficiently developed potential barrier.

When the tube current is finite, but smaller than the saturated current, the tube current is called space-charge limited. This situation occurs when the kinetic energy of the charged particles becomes zero somewhere between the emitter and the collector but part of the charged particles still reach the collector.

In the space-charge limited case a singularity in the space-charge density distribution occurs at the point where the kinetic energy becomes zero, since at that point the particle velocity is zero, while the current is finite. In contrast to the behavior of the space-charge distribution the space-charge density itself remains finite, due to the fact that the concept of density is related to a finite volume.

Although the calculation of the current characteristics of the vacuum diode can be carried out for various geometries, this discussion will be confined to a plane-parallel-geometry. The expression for the current density as a function of the voltage V_a applied between the emitter and collector as well as of their separation d is derived in the following way. The units used throughout this chapter are mks rationalized units.

In the general space-charge limited case there are two separate regions of interest between the emitter and the collector. These regions are called the α and β regions.

These regions (Fig. 2.1) are defined as follows:

α-region: The region between the emitter and the potential extreme, i.e., $0 < x < x_m$.

β-region: The region between the potential extreme and the collector, i.e., $x_m < x < d$.

Consider the condition in which negatively charged particles leave the emitter. Since the emitted current is J_o and a current J is collected, a current $(J_o - J)$ flows from a "virtual emitter", located at x_m, to the actual emitter. Corresponding to this

In the space-charge limited case a singularity in the space-charge density distribution occurs at the point where the kinetic energy becomes zero, since at that point the particle velocity is zero, while the current is finite. In contrast to the behavior of the space-charge distribution the space-charge density itself remains finite, due to the fact that the concept of density is related to a finite volume.

Although the calculation of the current characteristics of the vacuum diode can be carried out for various geometries, this discussion will be confined to a plane-parallel-geometry. The expression for the current density as a function of the voltage V_a applied between the emitter and collector as well as of their separation d is derived in the following way. The units used throughout this chapter are mks rationalized units.

In the general space-charge limited case there are two separate regions of interest between the emitter and the collector. These regions are called the α and β regions.

These regions (Fig. 2.1) are defined as follows:

α-region: The region between the emitter and the potential extreme, i.e., $0 < x < x_m$.

β-region: The region between the potential extreme and the collector, i.e., $x_m < x < d$.

Consider the condition in which negatively charged particles leave the emitter. Since the emitted current is J_o and a current J is collected, a current $(J_o - J)$ flows from a "virtual emitter", located at x_m, to the actual emitter. Corresponding to this

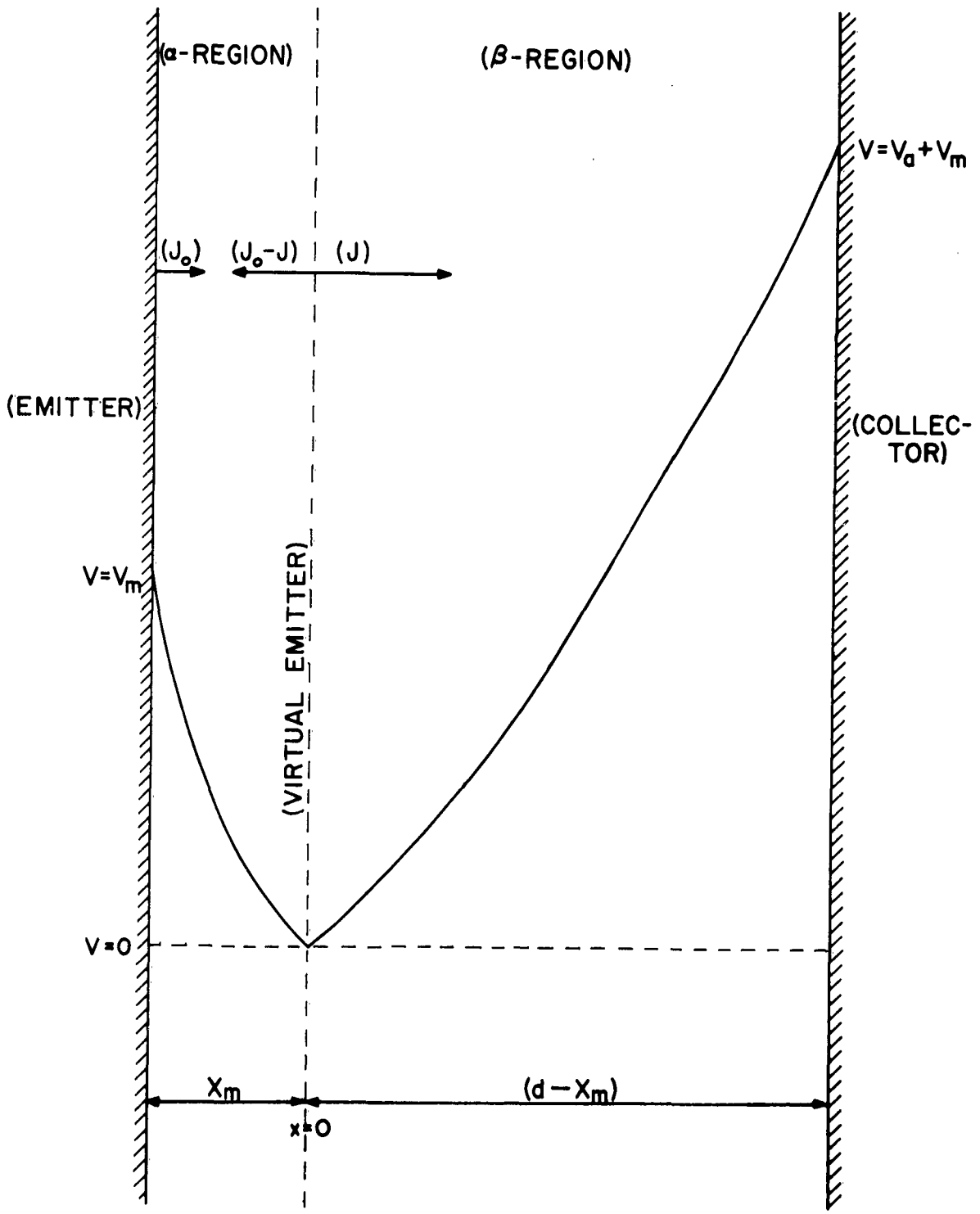

FIG. 2.1 POTENTIAL DISTRIBUTION IN A SPACE-CHARGE-LIMITED VACUUM DIODE

situation is a potential distribution of the form as shown in Fig. 2.1.

The velocity of the charged particles is zero at the potential extreme. Consequently, the magnitude of the velocity of the particles originating from both the actual emitter and the virtual emitter is the same at any point in the α-region. Therefore, the absolute value of the space-charge distribution in the α-region is given by

$$\left| \rho_\alpha(x) \right| = \left| \frac{J_o}{v(x)} \right| + \left| \frac{J_o - J}{v(x)} \right| = \left| \frac{2J_o - J}{v(x)} \right| = \frac{J_\alpha}{|v(x)|} , \quad 0 \leq x \leq x_m . \tag{2.1a}$$

In the β-region we have

$$\left| \rho_\beta(x) \right| = \left| \frac{J}{v(x)} \right| = \left| \frac{J_\beta}{v(x)} \right| , \quad x_m \leq x \leq d , \tag{2.1b}$$

where thus

$$J_\alpha = \left| 2J_o - J \right| , \tag{2.1c}$$

and

$$J_\beta = \left| J \right| . \tag{2.1d}$$

The velocity v(x) is equal to

$$v(x) = \left(\frac{2}{m} \, q \, V \right)^{1/2} , \tag{2.2a}$$

with

$$v(-x_m) = v_o \qquad (2.2b)$$

Obviously, the space-charge is negative for electrons (assumed in Fig. 2.1) and positive for positive ions.

As a consequence of the assumption of space-charge limited current, the potential distribution will have a maximum or minimum at a plane located between the emitter and collector. The electric field strength will thus be zero there. The magnitude of the depth (or height) of the potential barrier follows from (2.2) and reads

$$|V_m| = \frac{mv_o^2}{2|q|} \qquad (2.3)$$

According to expressions (2.1a - 2.1d), which furnish the space charge distributions in the α- and β-regions, the properties of these regions are simply given by Child's law for vacuum diodes satisfying the following conditions:

	α-Region	β-Region
Cathode Potential	0 volts	0 volts
Anode Potential	V_m volts	$(V_a + V_m)$ volts
Electric Field Strength at Cathode	0 volts/cm	0 volts/cm
Current Anode Spacing	x_m	$(d - x_m)$
Tube Current	J_α	J_β

The cathode of the α- and β-diodes coincide with the virtual emitter of our space-charge limited diode. The "anode" of the α-diode

is the emitter, while the "anode" of the β-diode is the collector. The applied potential between emitter and collector is V_a volts, and the spacing is equal to d. The electric field strength at the surface of the emitter (the anode of the α-tube) will be denoted by E_o.

The equations of interest relating to the α- and β-regions are easily found to be:

α-Region:

$$|2J_o - J| = \frac{c\,|V_m|^{3/2}}{x_m^2} \tag{2.4}$$

where

$$c = \frac{4\varepsilon_o}{9}\left[\frac{2|q|}{m}\right]^{1/2} \tag{2.5}$$

Thus

$$x_m = \frac{2}{3}\left(\frac{m\varepsilon_o}{2|q|\,|2J_o - J|}\right)^{1/2} v_o^{3/2} \tag{2.6}$$

From Eq. (2.4) the magnitude of the electric field strength at the emitter can be expressed in the following forms:

$$E_o = \left[\frac{6m}{|q|}\right]^{1/3}\left[\frac{|2J_o - J|}{\varepsilon_o}\right]^{2/3} x_m^{1/3} \tag{2.7}$$

$$E_o = \left[\frac{2m\,|2J_o - J|}{|q|\,\varepsilon_o}\right]^{1/2} v_o^{1/2} \tag{2.8}$$

$$E_o = \left[\frac{2|2J_o - J|}{\varepsilon_o} \left(\frac{2m}{|q|}\right)^{1/2} \right]^{1/2} |V_m|^{1/4} \qquad (2.9)$$

β-Region:

$$J = c \frac{|V_a + V_m|^{3/2}}{(d - x_m)^2} \qquad (2.10)$$

By taking the ratio of Eqs. (2.4) and (2.10) it is found that

$$\frac{x_m}{d} = \left[1 + \left(\frac{2|J_o|}{|J|} - 1 \right)^{1/2} \left(\frac{V_a}{V_m} + 1 \right)^{3/4} \right]^{-1} \qquad (2.11)$$

which is the expression derived by Langmuir.[1]

Figures 2.2 and 2.3 show plots of (x_m/d) versus $(|J_o|/|J|)$ for constant values of $(|V_a|/|V_m|)$ and (x_m/d) versus $(|V_a|/|V_m|)$ for constant values of $(|J_o|/|J|)$. In Fig. 2.4 the connection between the potential distribution and the space-charge density is indicated, as implied by Poisson's equation. From this figure it follows that a positive (negative) E_o can exist only when a negative (positive) space-charge is present in the collector region.

The set of Eqs. (2.3 - 2.11) give the complete description of the properties of a space-charge limited vacuum diode. For instance, with a given type of charged particle and known d, V_a, J_o and v_o the expressions (2.10) and (2.11) give x_m and the tube current J, while the value of the electric field strength at the emitter then follows from Eqs. (2.7 - 2.9).

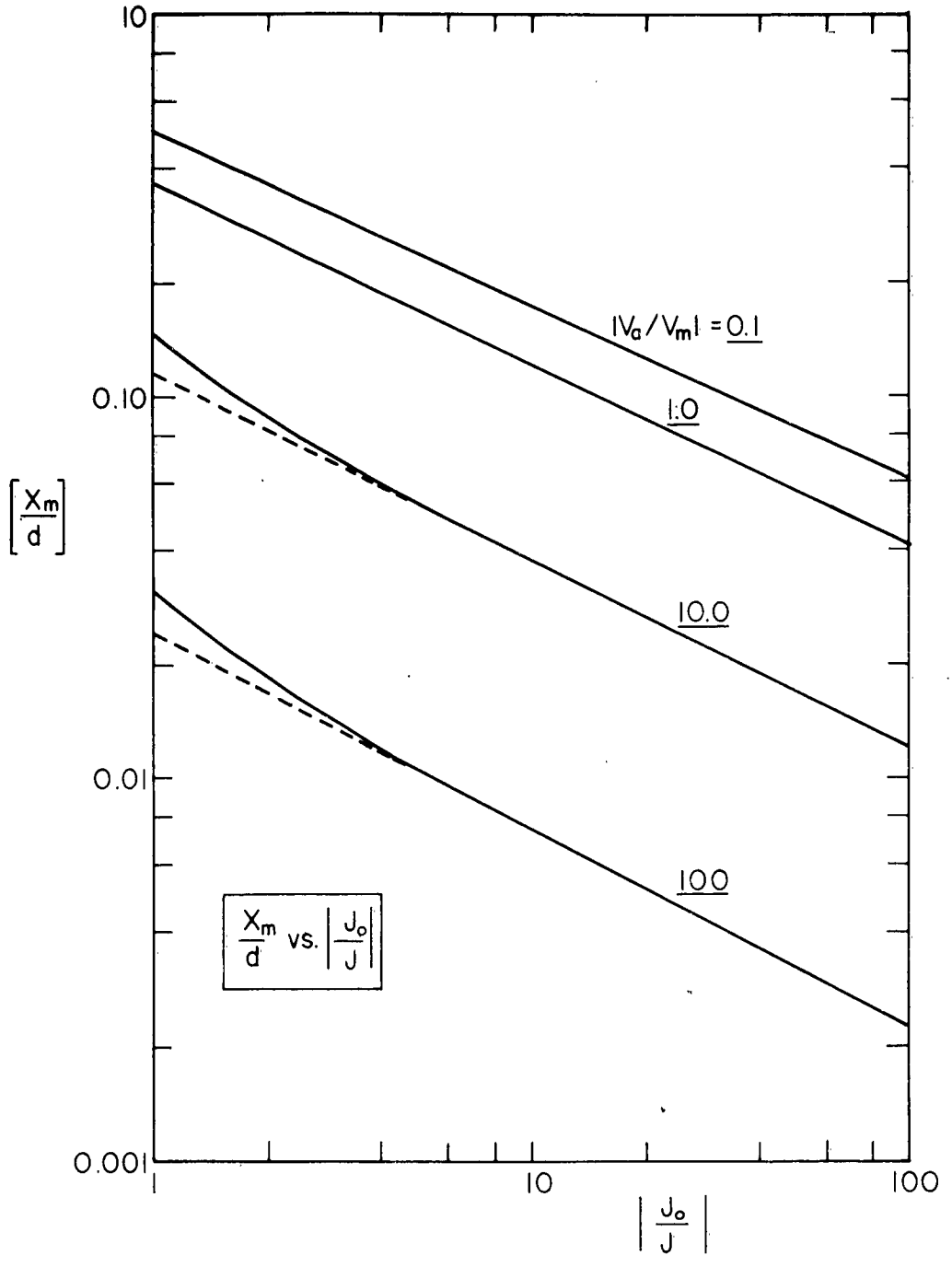

FIG. 2.2 $\left[\frac{X_m}{d}\right]$ AS A FUNCTION OF $\left|\frac{J_o}{J}\right|$ FOR CONSTANT $\left|\frac{V_a}{V_m}\right|$

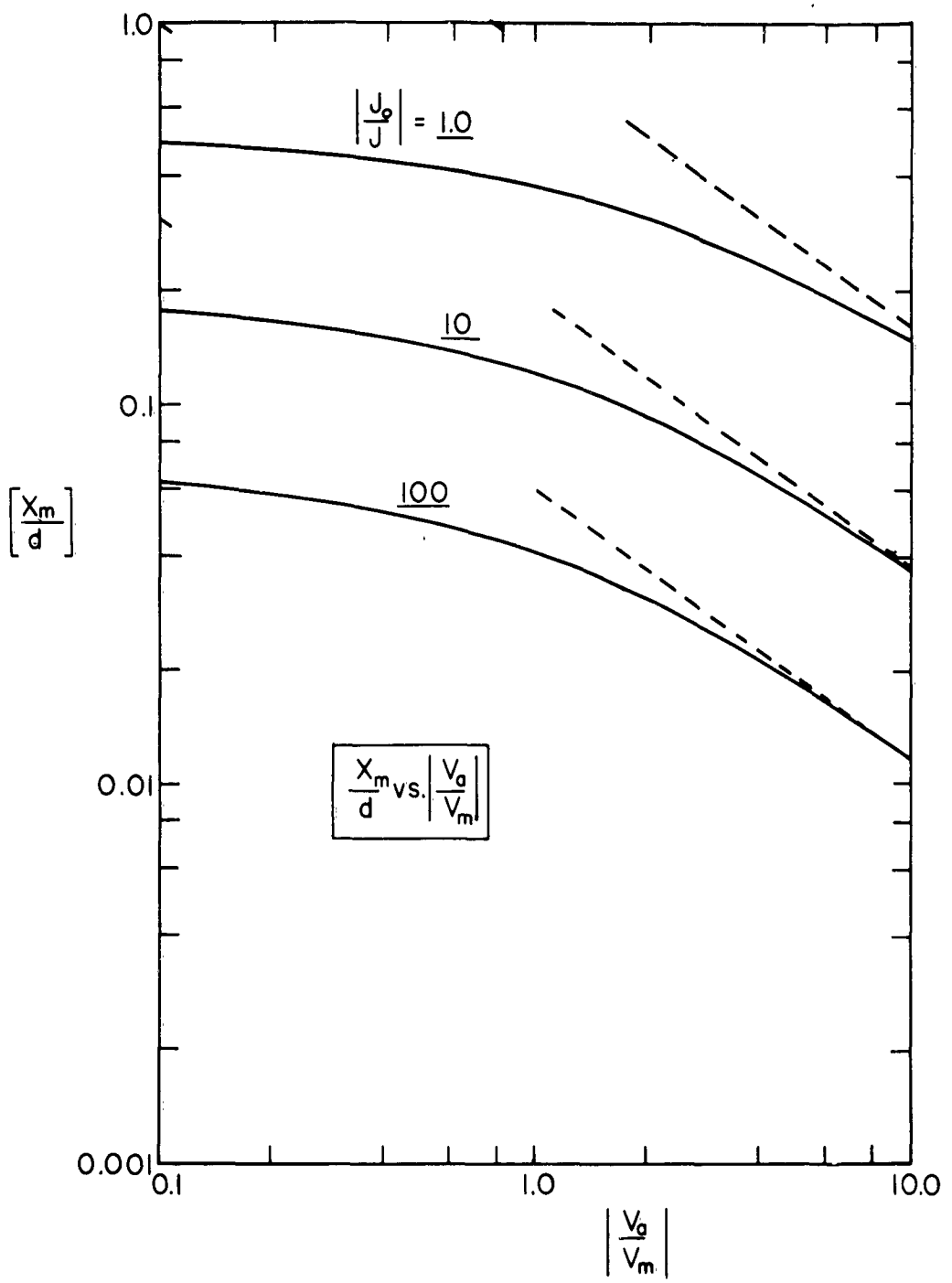

FIG. 2.3 $\left[\frac{X_m}{d}\right]$ AS A FUNCTION OF $\left|\frac{V_a}{V_m}\right|$ FOR CONSTANT $\left|\frac{J_o}{J}\right|$

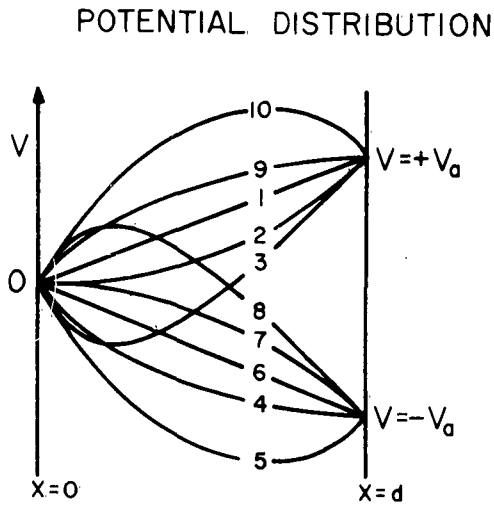

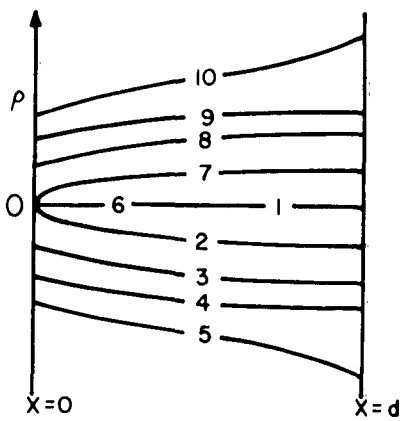

FIG. 2.4 THE RELATION BETWEEN THE POTENTIAL AND THE SPACE-CHARGE DISTRIBUTION

2.2.3 The velocity distribution method

The physical phenomena prevailing in a practical vacuum diode require that assumptions different from those of the preceding section be made to give an accurate expression for the diode current density. The previously used assumption that the charged particles leave the emitter with a monoenergetic velocity v_o does not apply for an actual vacuum diode. Instead the particles will leave the emitter with a velocity distribution, and the following assumptions are generally made:[1]

1) Only singly charged particles of one sign and mass leave the emitter.

2) The particles leave the emitter with velocities corresponding to a one-sided Maxwellian velocity distribution. The particles emitted with velocities between (v_x) and $(v_x + dv_x)$ contribute to the tube current density an amount

$$dJ = J_o \left(\frac{mv_x}{kT}\right) \exp\left(\frac{-mv_x^2}{2kT}\right) dv_x \quad , \qquad (2.12)$$

where J_o is the saturation current density, and T is the cathode temperature (in degrees Kelvin).

This situation has been discussed in the literature for the case of electrons, but it should be emphasized that the derivation of the expressions describing the diode properties do not depend on the particle mass or sign.

Here only the major steps leading to the various relations will be presented, since the detailed discussion can be found in the literature.

The following steps are used to obtain the expressions for the current density.

1) The differential space-charge density in the plane located a distance x away from the emitter is found to be

$$d\rho = \frac{-Jm}{kT} \exp \left[\frac{q(V - V_m)}{kT} - \frac{mv_x^2}{2kT} \right] dv \quad .$$

2) To simplify the calculations the following quantities are defined:

The normalized potential energy

$$\eta = \frac{q(V - V_m)}{kT} \quad ,$$

and the normalized velocity

$$u = \left(\frac{m}{2kT} \right)^{1/2} v_x \quad .$$

Thus

$$d\rho = - J \left(\frac{2m}{kT}\right)^{1/2} e^{\eta} e^{-u^2} \quad du \quad . \qquad (2.13)$$

3) The total space-charge density at x is obtained by integrating (2.13) over the proper range of velocities. Again the α- and β-regions are treated separately.

The β-region: $x_m \leq x \leq d$, where x_m is the position of the potential maximum, and d is the distance between the emitter and collector.

Since the integration limits are $\eta^{1/2}$ and infinity it follows that

$$\rho_\beta = -J\left(\frac{2m}{kT}\right)^{1/2} e^{\eta} \int_{\eta^{1/2}}^{+\infty} e^{-u^2}\, du = -J\left(\frac{\pi m}{2kT}\right)^{1/2} e^{\eta}\left[1 - \operatorname{erf}(\eta)^{1/2}\right] . \tag{2.14}$$

The α-region: $0 \leq x \leq x_m$.

Taking into account the contribution to the space-charge density of the charged particles reflected by the space-charge barrier it is found that

$$\rho_\alpha = -J\left(\frac{2m}{kT}\right)^{1/2} e^{\eta}\left[\int_0^{\infty} e^{-u^2}\, du + \int_0^{\eta^{1/2}} e^{-u^2}\, du\right]$$

or

$$\rho_\alpha = -J\left(\frac{\pi m}{2kT}\right)^{1/2} e^{\eta}\left[1 + \operatorname{erf}(\eta)^{1/2}\right] . \tag{2.15}$$

4) The expression for ρ_α and ρ_β are substituted Poisson's equation, yielding

$$\frac{d^2V}{dX^2} = \frac{J}{\varepsilon_o}\left(\frac{\pi m}{2kT}\right)^{1/2} e^{\eta}\left[1 \pm \operatorname{erf}(\eta)^{1/2}\right] .$$

5) This equation is then integrated to give

$$\left(\frac{d\eta}{d\zeta}\right)^2 = e^{\eta} - 1 \pm \left[e^{\eta} \operatorname{erf}(\eta)^{1/2} - 2\left(\frac{\eta}{\pi}\right)^{1/2}\right] = \Phi(\eta) , \tag{2.16}$$

where

$$\zeta = \left(\frac{Jq}{\varepsilon_o}\right)^{1/2} \frac{(2\pi m)^{1/4}}{(kT)^{3/4}} \quad (x - x_m) \quad . \tag{2.16a}$$

Thus the problem has been reduced to one of integration, since

$$\zeta = \int_o^{\eta} \left[\Phi(\eta)\right]^{-1/2} \, d\eta \tag{2.17}$$

gives J as a function of V, V_m, x_m, etc. An additional equation is obtained by realizing that the electric field strength is zero at the potential maximum or minimum. A closed form solution of this integral in terms of elementary functions is not available and numerical integration must be used to obtain a solution.

If $\eta \gg 1$, the following approximate solution is found:[1]

$$J = \frac{4\varepsilon_o}{9} \left(\frac{2|q|}{m}\right)^{1/2} \frac{|V_a - V_m|^{3/2}}{|d - x_m|^2} \left[1 + \frac{3}{2}\left(\frac{\pi kT}{|q|\,|V_a - V_m|}\right)^{1/2} + \cdots\right]$$

or

$$J \cong \frac{4\varepsilon_o}{9} \left(\frac{2|q|}{m}\right)^{1/2} \frac{|V_a - V_m|^{3/2}}{|d - x_m|^2} \quad . \tag{2.18}$$

Thus, when the collector potential is large compared to $(kT/|q|)$, the space-charge limited thermionic diode behaves as if the charged particles are emitted mono-energetically with velocity

$$v_o = \left(\frac{2qV_m}{m}\right)^{1/2} \quad .$$

2.2.4 Remarks about the use of the monoenergetic method when the charged particles have a velocity distribution

When the charged particles do not leave the emitter monoenergetically, but their velocities in the direction perpendicular to the emitter are distributed according to a velocity distribution $f(v_x)$, the two situations as shown in Fig. 2.5a and 2.5b may occur.

The situation in which $f(v_x)$ consists of a thermal emission distribution superimposed on a velocity v_o (the drift) is shown schematically in Fig. 2.5a. There exists for the space-charge limited case a potential barrier of magnitude V_m located a distance x_m from the emitter which reflects part, but not all, of the emitted particles. Associated with the "height" V_m of the potential barrier a critical velocity v_c exists, given by

$$v_c = \left[\frac{2}{m} q V_m\right]^{1/2} , \qquad (2.19)$$

so that particles emitted with a velocity in the α-velocity range, defined by

$$v_o < v < v_c , \qquad (2.20)$$

will be reflected back to the emitter, while particles in the β-velocity range, defined by

$$v > v_c , \qquad (2.21)$$

will be collected.

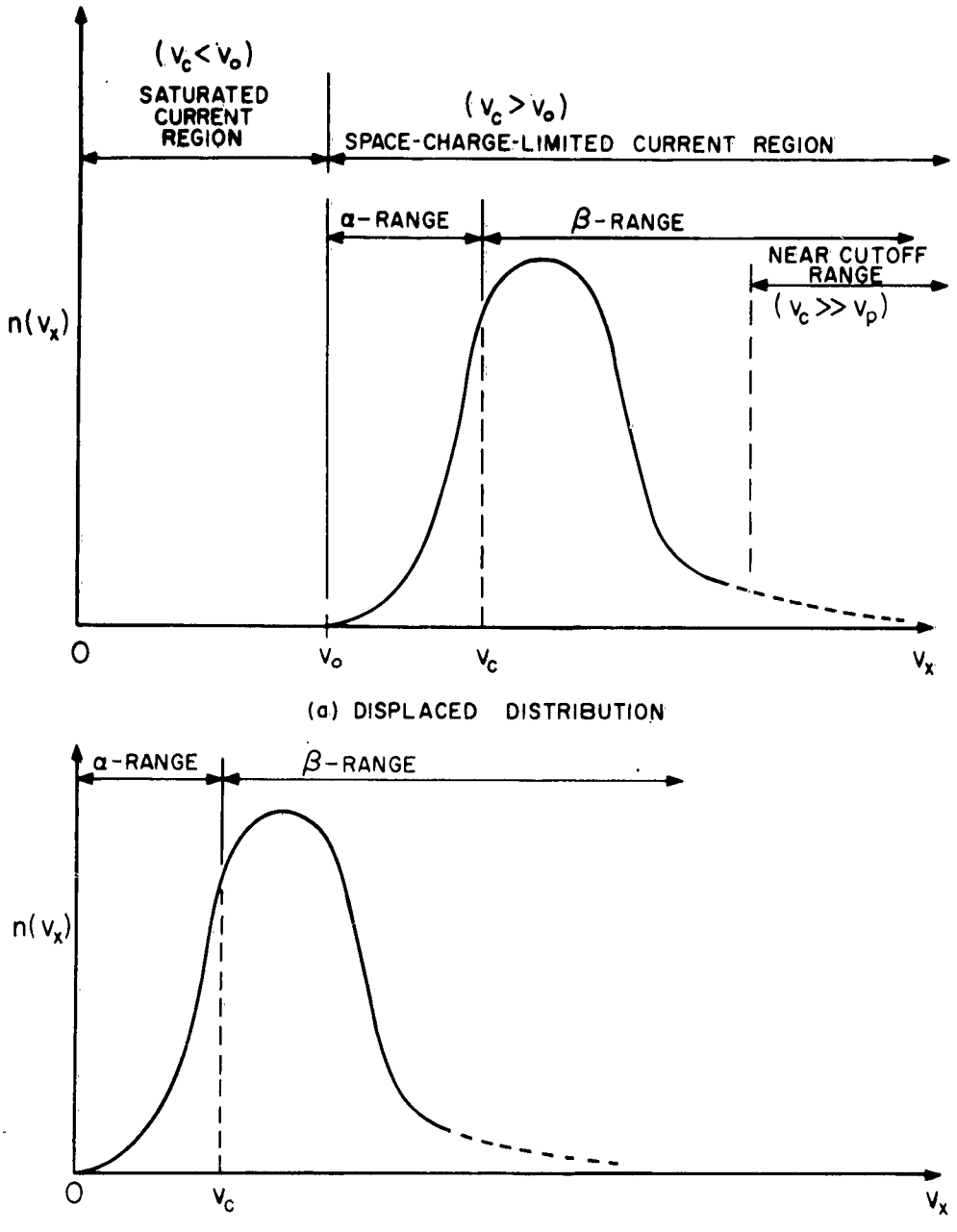

FIG. 2.5 THE RELATION BETWEEN THE VELOCITY DISTRIBUTION AND THE CURRENT COLLECTION PROPERTIES

Charged particles emitted with $v = v_c$ will have zero velocity at x_m, so that part of them will return to the emitter and part will be collected as follows from the monoenergetic method which was discussed in Sec. 2.2.2.

For a constant value of v_o, the magnitude of v_c, related to $|V_m|$ by (2.19), determines if the tube current is saturated or space-charge limited. Obviously, for $v_c < v_o$ the current is saturated, while for $v_c > v_o$ the current is always space-charge limited.

The broadness of the thermal velocity distribution function determines the magnitude of the change $|\Delta V_m|$ in $|V_m|$ for the transition from saturated tube current to nearly current cut-off. Evidently, when the thermal velocity distribution is narrow and v_o is not small, then the monoenergetic method will give a very good approximation for the value of $|V_m|$ and the formulae presented in Sec. 2.2.2 could be used.

However, when $v_o = o$, as shown in Fig. 4.5b, the relative change of $|V_m|$ when going through the various current collection regions is always large. Therefore, the use of the monoenergetic method with $|V_m|$ related to the average or most probable average particle velocity might lead to false results, especially for small values of the applied voltage.

2.2.5 Emission of two types of charged particles

The consequences of the emission of two different types of charged particles on the properties of the vacuum diode will be discussed very briefly in this section.

When the two types of particles have the same sign of charge, for instance two different groups of positive ions, a potential barrier could exist, which would limit the current through the vacuum diode in one of the following ways. The current due to charged particles of type 1 may be space-charge limited, while that due to the type 2 particles is saturated. The reverse situation can also exist, and when both types have the same emission energy both currents might be space-charge limited. Complete cut-off of the tube current occurs when none of the charged particles reach the collector. The last possibility of tube-current limitation is the condition in which the current due to one of the types is cut off while that due to the other is space-charge limited, or saturated.

When the two types of particles have opposite sign of charge, the situation becomes rather involved. Different types of potential barriers may exist and influence the magnitude of the tube current depending on the conditions at the emitter. The discussion of the various complications involved will be omitted here.

2.3 The Gas Diode

2.3.1 Introduction

When the charge carriers suffer collisions after leaving the emitter, their velocity is no longer given by expression (2.2). A rigorous derivation of the formulae describing the properties of a gas diode consists of a combination of the transport equations and Maxwell's equation. Here, however, relaxation effects between

the electric field strength E and the particle drift velocity $v_d(x)$ will be neglected, so that it can be assumed that

$$\left| v_d \left(E(x) \right) \right| = |K| \left| \frac{E(x)}{p_o} \right|^n , \qquad (2.22)$$

where $qE > o$ has to be satisfied. Here K is a proportionality factor relating the drift velocity to the electric field strength, n is the number determined by the type of charged particles, the type of gas and the E/p_o range, and p_o is the gas pressure.

Moreover, it will be assumed that K does not depend on E/p_o, i.e., it is independent of the charged particle energy. This assumption will be valid for certain ranges of E/p_o. The values of K and n are given in Table 2.1, presented in the next section, for electrons moving in various gases.

This derivation of the tube current as a function of various tube parameters will be carried out in the next section for the situation in which the charged particles have, at each location inside the tube, identical velocities, the value of which will depend on the location.

It should be realized that this is a stronger assumption than that relating to monoenergetic emission velocities, since the particle collisions tend to broaden the velocity distribution of the emitted charge carriers.

2.3.2 The monoenergetic method

The most interesting current collection region is the space-charge limited region. Again, the α- and β-regions, as defined in Sec. 2.2.2 for the vacuum diode, have to be discussed

separately. In this section the formulae relating to the β-region will be derived. As a consequence of the impossibility to apply the relation (2.22) to the retarding region (α-region), a special section will be devoted to the possible approach of taking into account the influence of particle collisions on the α-region properties.

The β-region is characterized by zero field strength at the virtual emitter which is located at a distance $(d - x_m)$ from the collector, while this collector has a potential $(V_a - V_m)$ with respect to the virtual emitter. Thus V_a is the voltage applied between actual emitter and collector when taking the emitter to be at zero potential, and V_m is the magnitude of the potential barrier.

As a consequence of the monoenergetic velocity assumption, combined with the assumed validity of relation (2.22) the formulae relating to the β-region are derived easily as follows:

The space-charge relation,

$$\rho(x) = \frac{J}{v(x)} \quad ,$$

and expression (2.22) inserted in Poisson's equation

$$\frac{dE(x)}{dx} = \frac{\rho(x)}{\epsilon} \quad .$$

The resulting equation is integrated over the appropriate E range (o - E) and x-range $(x_m - x)$. This yields

$$|E| = \left[\frac{(n+1)\ p_o^{\,n}\ J}{\varepsilon K}\right]^{1/(n+1)} (x - x_m)^{1/(n+1)} \quad . \tag{2.23}$$

Integrating expression (2.23) over the total voltage range $(V_m - V_a)$ and x-range $(x_m - d)$ gives the formula for the tube current, which reads

$$J = \frac{\varepsilon K}{(n+1)p_o^{\,n}} \left[\frac{n+2}{n+1}\right]^{n+1} \frac{|V_a - V_m|^{n+1}}{(d - x_m)^{n+2}} \quad . \tag{2.24}$$

In order to be able to apply this relation to an actual gas diode it is necessary to use the n-value as well as the K-value valid for the gas and the E/p-range of interest. The data referring to electrons are given in Table 2.1.

2.3.3 The loss of directed particle velocity in the retarded field region

In the retarded field region, i.e., the α-region of the gas diode, the directed emission velocity of the charged particles decreases, due to the combined effect of two mechanisms, i.e., a) transfer of the energy of the directed motion to the retarding field and b) the randomization of directed velocity due to elastic collisions between the charged particles and the gas atoms.

As a consequence of the presence of gas atoms, which thus adds to the loss mechanism of directed velocity, the distance from the emitter at which the average directed velocity is zero will be smaller in general than the corresponding distance found in the case of a vacuum diode.

TABLE 2.1

THE VALUES OF n AND K FOR VARIOUS E/p_o RANGES IN HELIUM, NEON, ARGON, HYDROGEN AND NITROGEN

Gas	n	K $\frac{cm}{sec}\left(\frac{cm(Torr)}{volts}\right)^n \times 10^6$	E/p_o - Range $\frac{volts}{cm(Torr)}$
Helium	1.0	7.0	10^{-4} - 10^{-2}
	0.5	0.8	10^{-2} - 1.0
Neon	0.5	1.0	10^{-4} - 4×10^{-3}
	0.4	0.8	4×10^{-3} - 0.4
	1.1	1.6	0.4 - 1.0
Argon	1.0	40.0	10^{-4} - 5×10^{-4}
	1.6	5,000	5×10^{-4} - 10^{-3}
	0.25	0.4	10^{-3} - 1.0
Hydrogen	1.0	5.0	10^{-4} - 8×10^{-2}
	0.44	1.0	8×10^{-2} - 1.0
	0.64	1.0	1.0 - 10
Nitrogen	1.0	10	10^{-4} - 2×10^{-2}
	0.33	0.8	2×10^{-2} - 1
	0.75	0.8	1.0 - 10

The energy "gain" per unit time of the directed energy $u_d = mv_d^2/2$ due to the retarding electric field, so that $qE < o$, is equal to qv_dE, while the rate of change in v_d due to collisions is equal to $-\nu_m v_d$, provided the collision frequency ν_m for momentum

transfer is independent of the charged particle energy.[9] Under these conditions the rate of change in the magnitude of v_d is given by

$$\frac{dv_d(x)}{dt} = \frac{q}{m} E(x) - \nu_m v_d(x) \qquad (2.25)$$

Equation (2.25) is one of the set of equations describing the properties of the α-region. The solution of this set of equations will give $v_d(x)$, $E(x)$ as well as E_o. When $v_d(x)$ can be obtained as a function of x, the location x_m of the minimum or maximum of the potential barrier can be found by setting $v_d(x) = o$. Calculating the value of V(x) at $x = x_m$ then yields the value for V_m. Substitution of x_m and V_m into (2.24) gives the relation between the tube current J and the gas diode parameters. This problem is mathematically very involved. Therefore, here, the two following limiting cases will be considered.

a) No collisions in the α-region

When the charges leaving the emitter suffer no collisions during their traversal through the α-region, the equations given in Sec. 2.2.2 referring to the α-region of the vacuum diode can be utilized. It should be realized that for the current J to be substituted in these equations expression (2.24) has to be used.

b) The effect of the retarding field can be neglected

Substituting $E(x) = 0$ in Eq. (2.25) and assuming ν_m to be constant the solution for $v_d(t)$ is

$$v_d(t) = v_d(0)\, e^{-\nu_m t} \quad , \tag{2.26}$$

so that

$$x_m = v_d(0) \int_0^\infty e^{-\nu_m t}\, dt = \frac{v_d(0)}{\nu_m} \tag{2.27}$$

Due to the neglect of the retarding field influence, the value given by (2.27) for x_m will be larger or equal to the actual value of x_m.

The situation in which more than one type of charged particle leaves the emitter will not be discussed here. The remarks about the applicability of the monoenergetic method when the charged particles have a velocity distribution while moving through the gas diode are analagous to those for the vacuum diode as discussed in Sec. 2.2.4. In Table 2.2 the various quantities of importance for the operation of the vacuum and gas diode are compared. Two important cases, i.e., n = 1/2 and n = 1, are chosen for the gas diode for purposes of comparison.

TABLE 2.2

A COMPARISON OF THE VACUUM AND GAS DIODE

	Vacuum Diode	Gas Diode	Gas Diode
	$V_b = V_a - V_m$ $\ell = x - x_m$ $D = d - x_m$	$V_b = V_a - V_m$ $\ell = x - x_m$ $D = d - x_m$ $n = 1$	$V_b = V_a - V_m$ $\ell = x - x_m$ $D = d - x_m$ $n = 1/2$
Current Density, (J)	$\frac{4\epsilon_o}{9D^2}\left(\frac{2qV_b}{m}\right)^{1/2}$	$\frac{9\epsilon K V_b^2}{8p_o D^3}$	$\frac{2\epsilon K}{3}\left(\frac{5^3 V_b^3}{3^3 p_o D^5}\right)^{1/2}$
Potential, (V)	$\left(\frac{3^4 m J^2 \ell^4}{2^5 \epsilon_o^2 q}\right)^{1/3}$	$\left(\frac{8p_o J \ell^3}{9\epsilon K}\right)^{1/2}$	$\frac{3}{5}\left(\frac{9p_o J^2 \ell^5}{4\epsilon^2 K^2}\right)^{1/3}$
Electric Field, (E)	$\left(\frac{6mJ^2\ell}{q\epsilon_o^2}\right)^{1/3}$	$\left(\frac{2p_o J \ell}{\epsilon K}\right)^{1/2}$	$\left(\frac{9p_o J^2 \ell^2}{4\epsilon^2 K^2}\right)^{1/3}$
Charge Density, (ρ)	$\left(\frac{2\epsilon_o m J^2}{9q\ell^2}\right)^{1/3}$	$\left(\frac{\epsilon p_o J}{2K\ell}\right)^{1/2}$	$\left(\frac{2\epsilon p_o J^2}{3K^2\ell}\right)^{1/3}$

References

1. I. Langmuir, Phys. Rev. 21, 419 (1923).

2. W. Schottky, Phys. Zeits. 15, 526, 624 (1914).

3. P. S. Epstein, Verh. d. Deutsch. Phys. Gesell. 21, 85 (1919).

4. P. C. Fry, Phys. Rev. 17, 441 (1921); 22, 445 (1923).

5. I. Langmuir and K. T. Compton, Rev. Mod. Phys. 3, 191 (1931).

6. W. B. Davenport, Jr. and W. L. Root, Random Signals and Noise, McGraw-Hill (1958) pp. 129-135.

7. C. E. Fay, A. L. Samuel and W. Shockley, "On the Theory of Space Charge Between Parallel Plane Electrodes," the Bell System Technical Journal 17, 49-79 (1938).

8. J. L. Pack and A. V. Phelps, Phys. Rev. 121, 798-806 (1961).

9. W. P. Allis, "Motions of Ions and Electrons," Tech. Rep. 299, p. 16, Research Lab. of Electronics, M.I.T., June 13, 1956.

Chapter 3

Previous Studies

3.1 Studies Relating to Child's Law

Child's Law[1] valid for space-charge limited conditions in a high vacuum diode was derived in 1911. Since that time countless verifications of his relationship have been made. Some of the first measurements carried out to check the validity of Child's Law were made by Langmuir.[2-5] This author extended and generalized the formula derived by Child. The theoretical and experimental details of thermionic emission in vacuum diodes are still being refined and verified.[6] However, it seems certain that in the monoenergetic case the fundamental current-voltage-spacing relationship for the space-charge limited high vacuum diode is given by

$$I = \frac{CV}{d^2}^{3/2} , \qquad (3.1)$$

where

$$C = \frac{4\varepsilon_o}{9} \left[\frac{2q}{m}\right]^{1/2} \qquad (3.2)$$

V is the applied potential, and d is the emitter to collector spacing.

3.2 Studies Relating to the Gas Diode

Although the importance of the high pressure diode has been realized for a long time a relatively small number of fundamental

studies concerning the relationship between current, voltage, and spacing have been made for this type of diode.

A notable study in recent years concerning the characteristics of high pressure gas diodes is the one made by Forman.[7] The object of his studies was to show that the current in a gas diode varies as $V^{3/2}$ instead of V^2 as derived by Cobine.[8] Forman's measurements were obtained from cylindrical diodes having heated emitters in which the emitter to collector spacing could not be varied. The current density was measured as a function of the type of gas, the gas pressure and the applied potential.

This author assumed that the velocity of the electrons was determined by mobility according to the relation

$$v_d = K \left(\frac{E}{p}\right)^{1/2} .$$

The value n = 1/2 was based on a theoretical analysis of the elastic scattering of electrons in a high pressure gas.[9,10] However, in spite of the appeal of a theoretical value for n, more realistic information concerning the drift velocities of electrons in helium, neon, argon, hydrogen and nitrogen can be found from experimental data.[11] The constant value n = 1/2, as used by Forman, is a dangerous simplification since Table 2.1 shows that the appropriate value for n depends on the type of gas and the (E/p_o) range, assuming, of course, that the electron velocity is determined by the mobility over the entire emitted-collector gap. Moreover, this author neglects the unavoidable presence, and therefore influence of the α-region in the space-charge limited situation.

References

1. C. D. Child, Phys. Rev. 32, 492 (1911).
2. I. Langmuir, Phys. Rev. 21, 419 (1923).
3. I. Langmuir and K. B. Blodgett, Phys. Rev. 22, 347 (1923).
4. I. Langmuir and K. B. Blodgett, Phys. Rev. 23, 49 (1924).
5. I. Langmuir and K. T. Compton, Rev. Mod. Phys. 3, 251 (1931).
6. W. B. Nottingham, "Thermionic Emission," Tech. Report 321, (1956), Res. Lab. of Electronics, M.I.T.
7. R. Forman, Phys, Rev. 123, 1537 (1961).
8. J. D. Cobine, "Gaseous Conductors," Dover, 128-129 (1958).
9. P. M. Morse, W. P. Allis, and E. S. Lamar, Phys. Rev. 48, 412 (1935).
10. A. von Engel, "Ionized Gases," Oxford University Press, New York, 104 (1955).
11. J. L. Pack and A. V. Phelps, Phys. Rev. 121, 798 (1961).

Chapter 4

Equipment

4.1 Introduction

The main components of the equipment used for the studies to be presented in Chapter 6 are a) the experimental tube, b) the vacuum system used for pumping and filling the tube and c) the electronic components necessary for measuring current and voltage.

These main components along with the cleaning and assembly techniques will be described in separate sections, while the measuring method will be discussed in Chapter 5.

4.2 The Experimental Tube

Drawings of the experimental tube sections are shown in Figs. 4.1a and 4.1b, whereas a picture of the tube is given in Fig. 4.2. The tube has two main sections. In one section free electrons and ions are produced by means of a dc gaseous discharge which is maintained between the cathode (Ca) and the planar screen (Sl) which is parallel to the cathode. The other section contains a collector (Co) which is parallel to (Sl). The first section thus acts as the production region for the charged particles. The second section is used to study the motion of these particles in a gaseous environment.

Metal flanges (Varian #V-10040 and #V-10041), with copper gasket seals, are an integral part of the tube. They were used to allow access to the inside of the tube so that changes in the tube design could be easily made. The various parts of the tube will be discussed in more detail in the next sections.

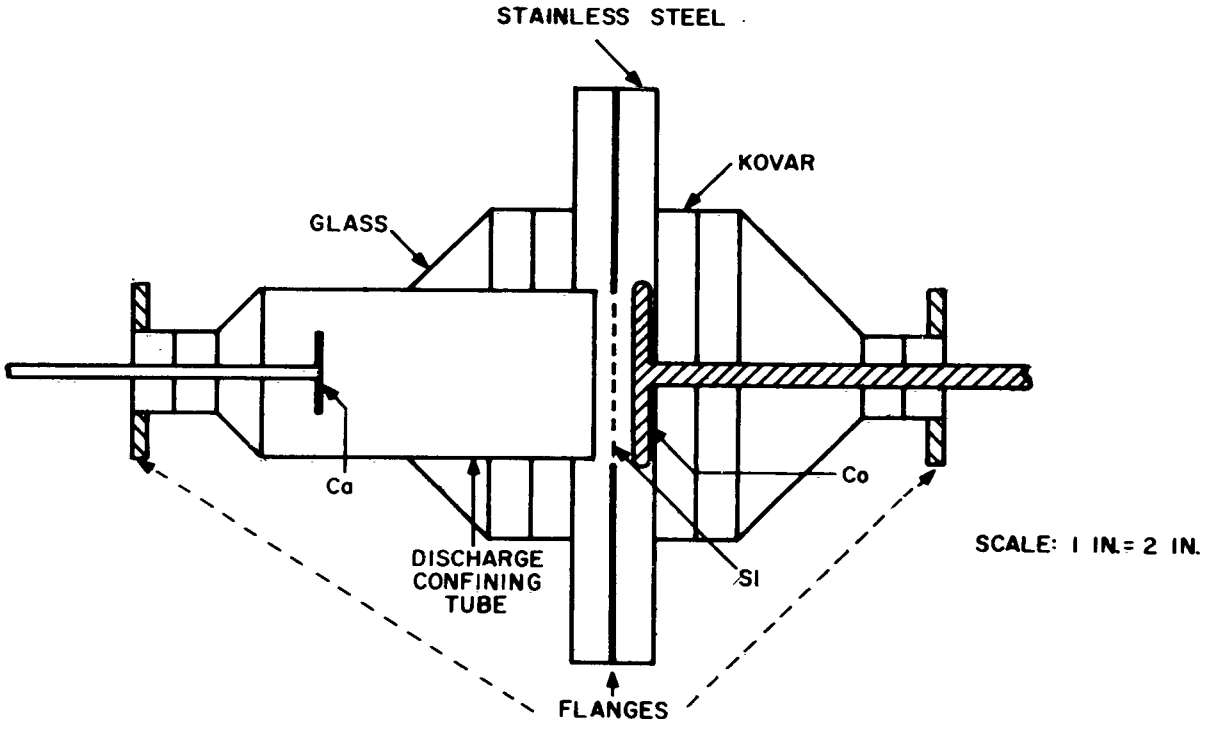

FIG. 4.1a EXPERIMENTAL TUBE (DISCHARGE AND COLLECTOR SECTIONS)

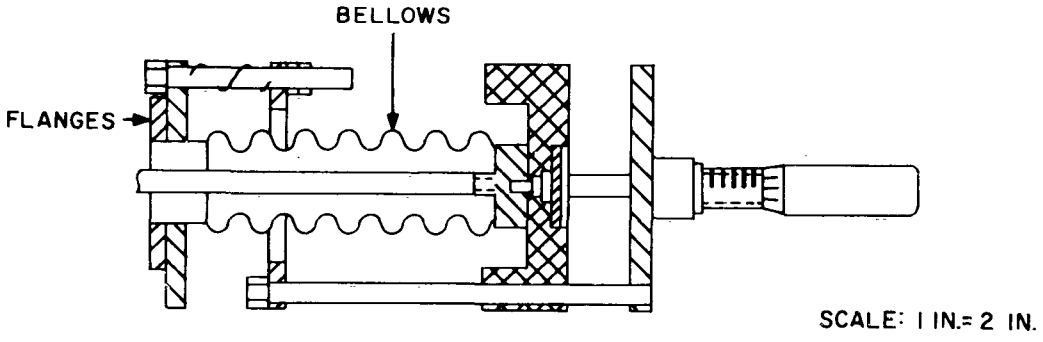

FIG. 4.1b EXPERIMENTAL TUBE(DRIVER SECTION)

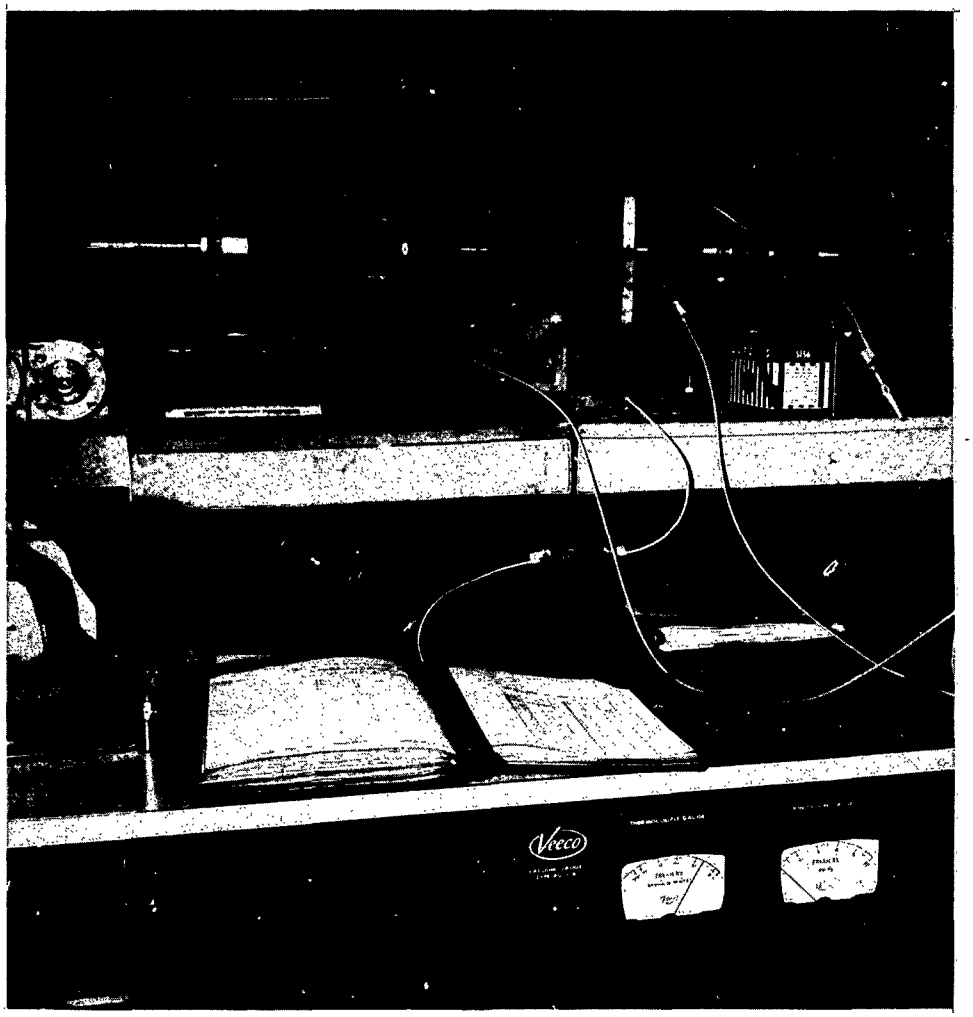

Fig. 4.2 The Experimental Tube

4.2.1 The adjustment of the cathode

The distance between the cathode (Ca) and the screen (S1) as well as their parallelism were found to be important factors for obtaining the desired properties of the screen which acts as emitter for the collector region of the tube. Therefore, a cathode positioner was designed that would allow the cathode to be accurately placed parallel and at a given distance from the screen.

The positioner consists of two units, i.e., a driver unit and a bellow unit. Since it would be impractical to machine all the tube elements so that the cathode would be parallel to the screen when the tube is finally assembled, the driver unit was provided with three thumb nuts that allow the cathode to be adjusted to be parallel to the screen. The spacing between the cathode and the screen is varied by using a micrometer head. The bellow unit was made by welding a stainless steel bellow onto a standard Varian #954-0010 flange. The other end of the bellow was welded onto a stainless steel block provided with an #8-32 stud and an #8-32 tapped hole for connection to the cathode rod and the driver unit, respectively.

By using the cathode positioner the spacing can be varied 50 mm with a positioning accuracy of $\pm$ 5 microns. The technique used for adjusting the cathode to be parallel to the screen allows the cathode to be brought into a position arbitrarily parallel to the screen. Under normal operating conditions the maximum angle between the planar cathode and the screen (assuming a perfectly flat screen) is adjusted to be less than 0.5 degrees.

4.2.2 The discharge cathode

The two following types of cathodes were used:

a) The hollow cathode

Initially a molybdenum cylindrically shaped hollow cathode was employed because it was felt that as much current as possible would be needed in the discharge section to allow measurable amounts of current to be obtained in the collector region. The fact that the diameter of the hollow cathode was small in relation to the screen diameter caused the discharge to be nonuniform across the surface of the screen. Hence, the results obtained with this type cathode are difficult to interpret.

A drawing of the hollow cathode is given in Fig. 4.3.

b) The planar cathode

A drawing of the planar cathode used during later studies is shown in Fig. 4.4. This cathode is made of type #303 stainless steel. By using the planar cathode in conjunction with the cathode positioner, very accurate and interpretable measurements relating to the discharge region could be obtained. At the present time a nickel cathode, of the type shown in Fig. 4.4., is being used.

4.2.3 The collector section

Two types of collectors have been used. By using a collector positioner similar to the cathode positioner the collector could be moved over a distance of 25 mm with an accuracy of 0.005 mm. The first type of collector used was a planar disc two inches in diameter similar to the cathode shown in Fig. 4.4. The second type of collector is a screened collector. It consists of a screen

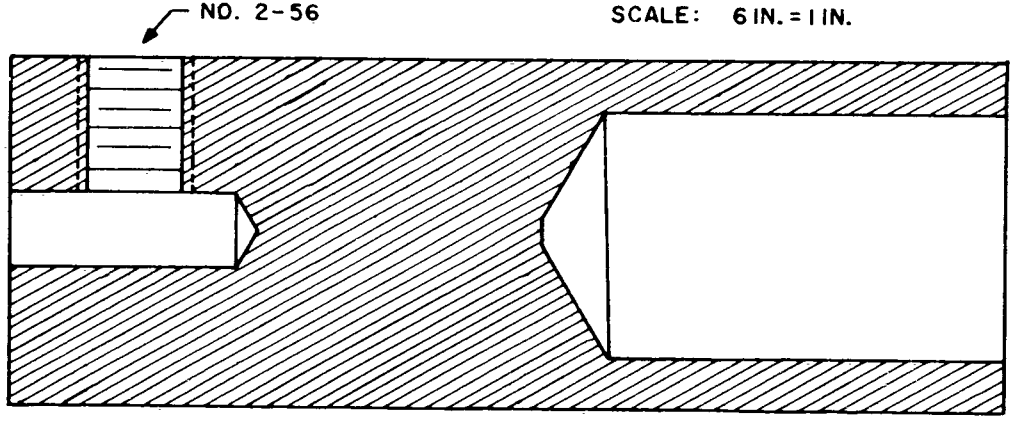

FIG. 4.3 HOLLOW CATHODE NO. 1

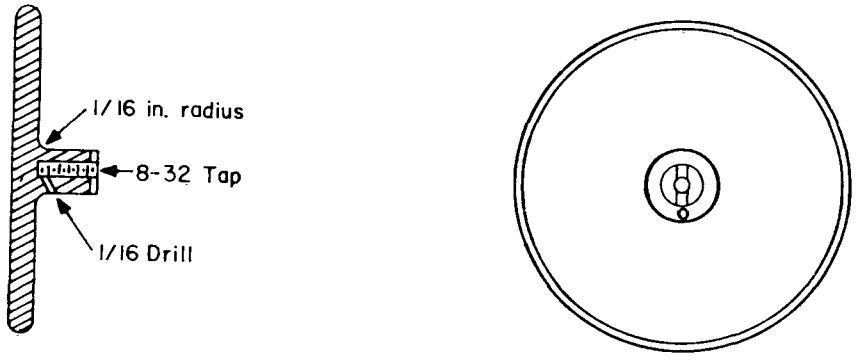

FIG. 4.4 PLANAR CATHODE

(S2) insulated electrically from the collector (Co) and fixed at a distance of one millimeter in front of it. The screened collector is shown in Fig. 4.5.

4.2.4 The discharge screen holder

The screen that was first used in this tube consisted of a fine mesh nickel screen bonded to a copper disc with a one inch diameter hole drilled in the center of it. This screen is shown in Fig. 4.6. The copper disc thus served the dual purpose of holding the screen in place and providing the vacuum seal for the flanges. This type of screen was found to deform slightly as a consequence of the bake-out procedure used for cleaning the tube. Another disadvantage of this type of screen was that it could only be used once.

A different type of screen holder is presently being used, and is shown in Fig. 4.7. This holder can be used repeatedly and screens having any mesh size and thickness can be mounted on it. This type of holder has proven to be very satisfactory in keeping the screen flat and little or no deforming has been observed.

4.3 Vacuum Station

A diagram of the vacuum system is shown in Fig. 4.8 and a photograph of the system is given in Fig. 4.9. The vacuum system can be baked out at temperatures up to 400°C. The tube is filled with gas at the required pressure, and all measurements can be carried out while the tube is connected to the vacuum system.

Two traps, of the type described by Biondi,[1] are filled with Linde type A molecular seive and are used to reduce the vapor

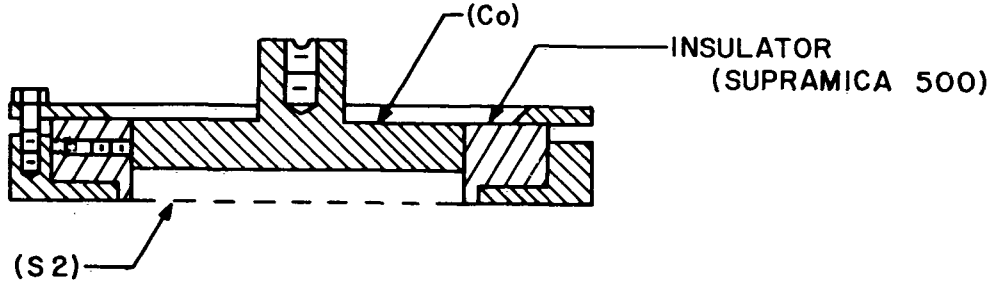

FIG. 4.5 COLLECTOR ASSEMBLY

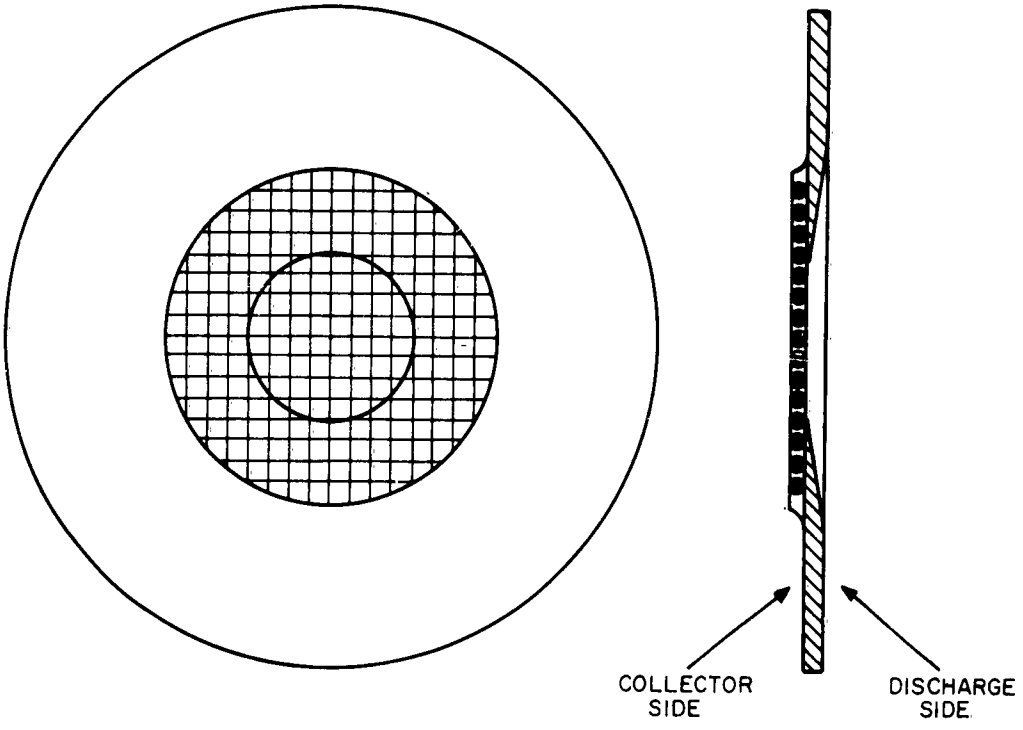

FIG. 4.6 SCREEN HOLDER (S1)

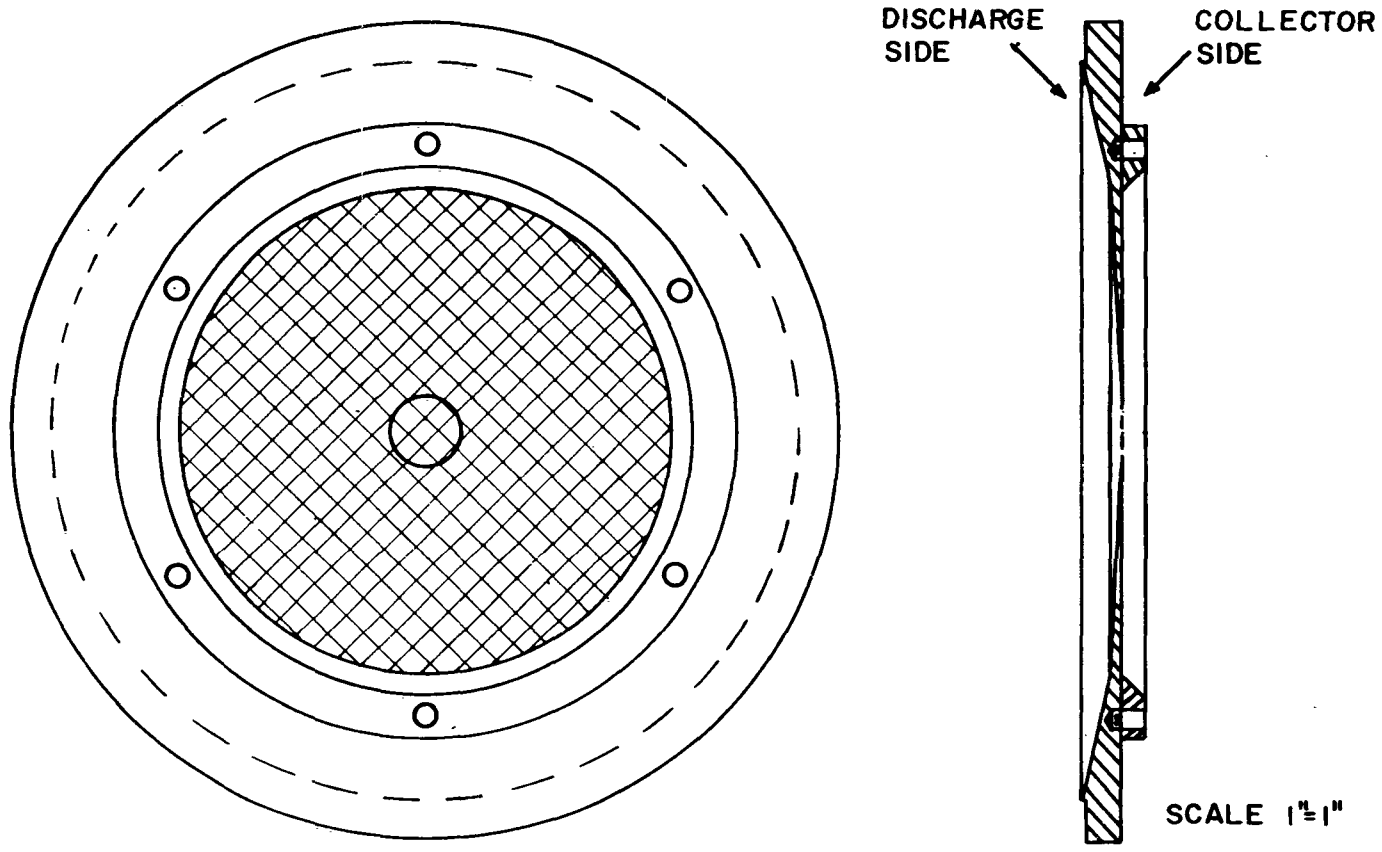

FIG. 4.7 SCREEN HOLDER (SI)

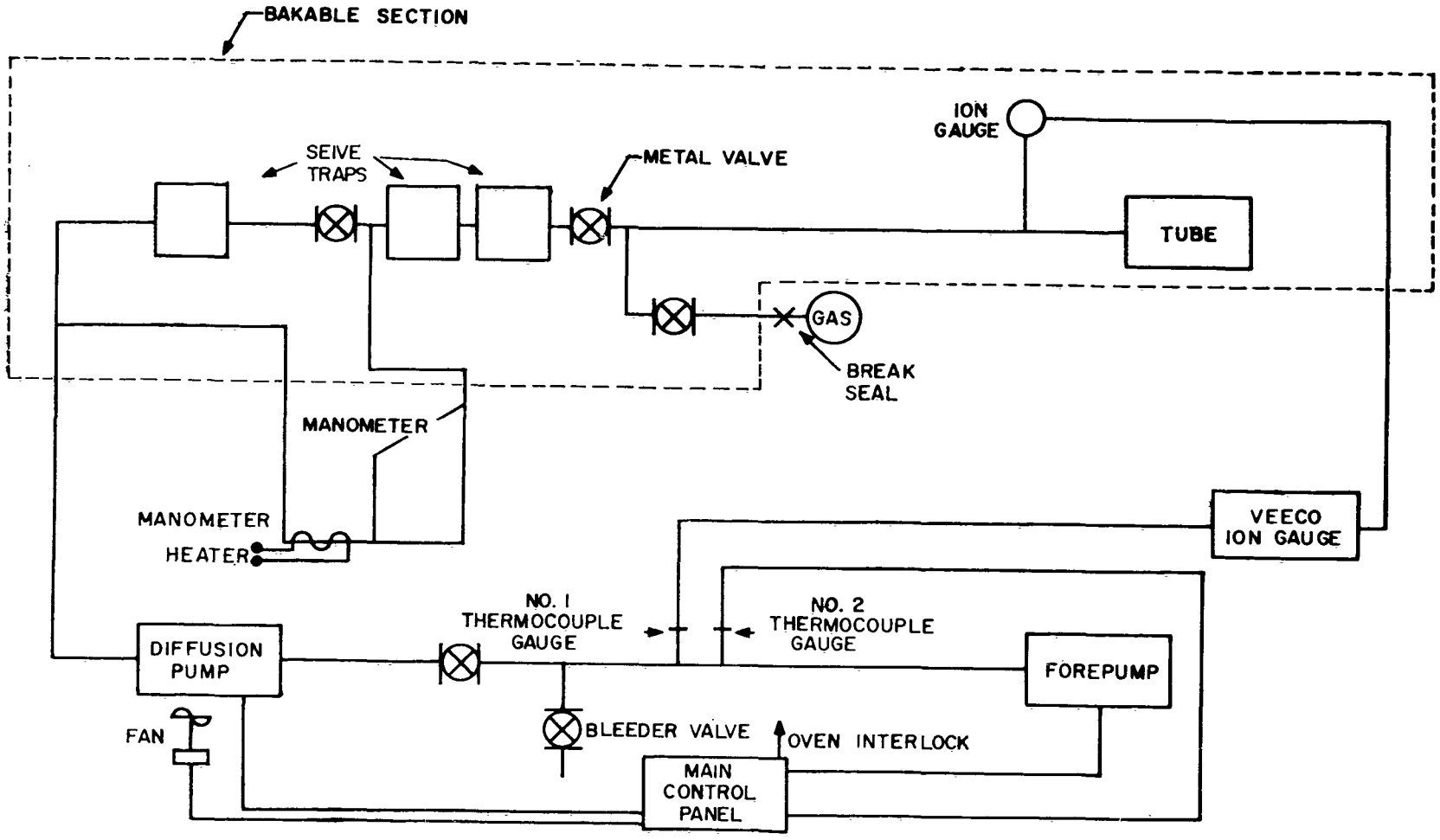

FIG. 4.8 VACUUM SYSTEM

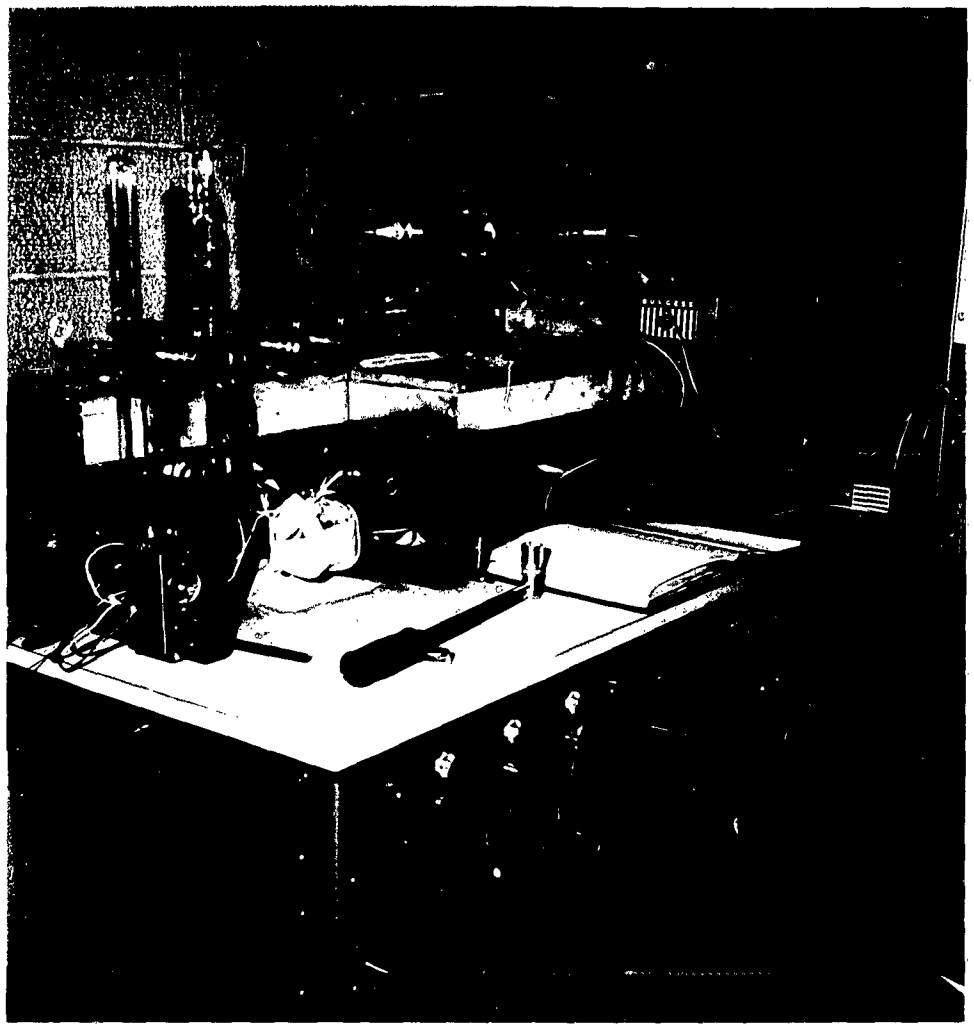

Fig. 4.9 The Vacuum System

pressure of the manometer and diffusion pump oil in the system. These traps are located below the transite platform and can be cooled with liquid nitrogen. The high vacuum pressure is measured by a Veeco #RG-31A high vacuum gauge. The gas pressure in the tube is measured with an oil monometer[2] filled with "Octoil S".

The vacuum system is equipped with automatic controls that will shut off the current to the diffusion pump and the bake-out ovens when the forepump pressure increases appreciably during the bake-out procedure due to a malfunction of the system. This reduces the damage inflicted to the experimental tube as well as the vacuum system. The oven and main control circuits are shown in Figs. 4.10 and 4.11.

4.4 Electronic Equipment

The studies to be reported required only the measurement of voltages and currents between the various elements of the tube. A block diagram of the complete measuring circuit is shown in Fig. 4.12. The instruments used are listed in Table 4.1.

4.5 Cleaning and Assembly of the Experimental Tube

Before the tube is assembled the various tube components are thoroughly degreased and cleaned. Then the tube is evacuated and the molecular sieve traps are outgassed at a temperature of about 400°C, while these traps remain separated from the tube. After sufficient outgassing and cooling of these traps the tube is reconnected to the diffusion pump, and the complete system is baked at a temperature of about 350°C until the system pressure is sufficiently low. After a bake-out point of eight hours at this

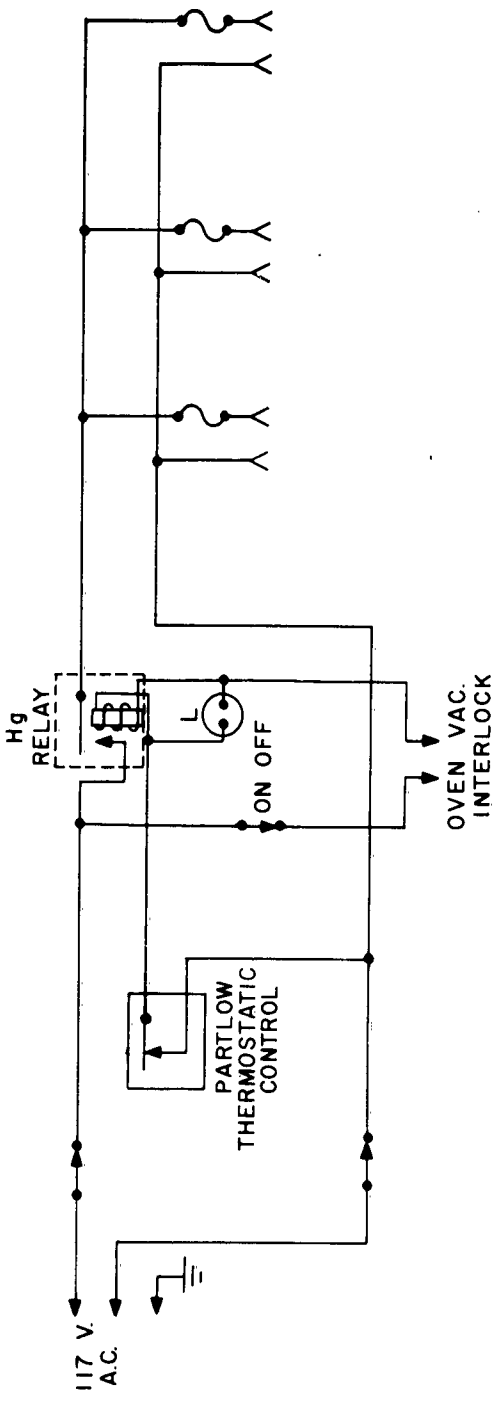

FIG. 4.10 OVEN CONTROL PANEL CIRCUIT

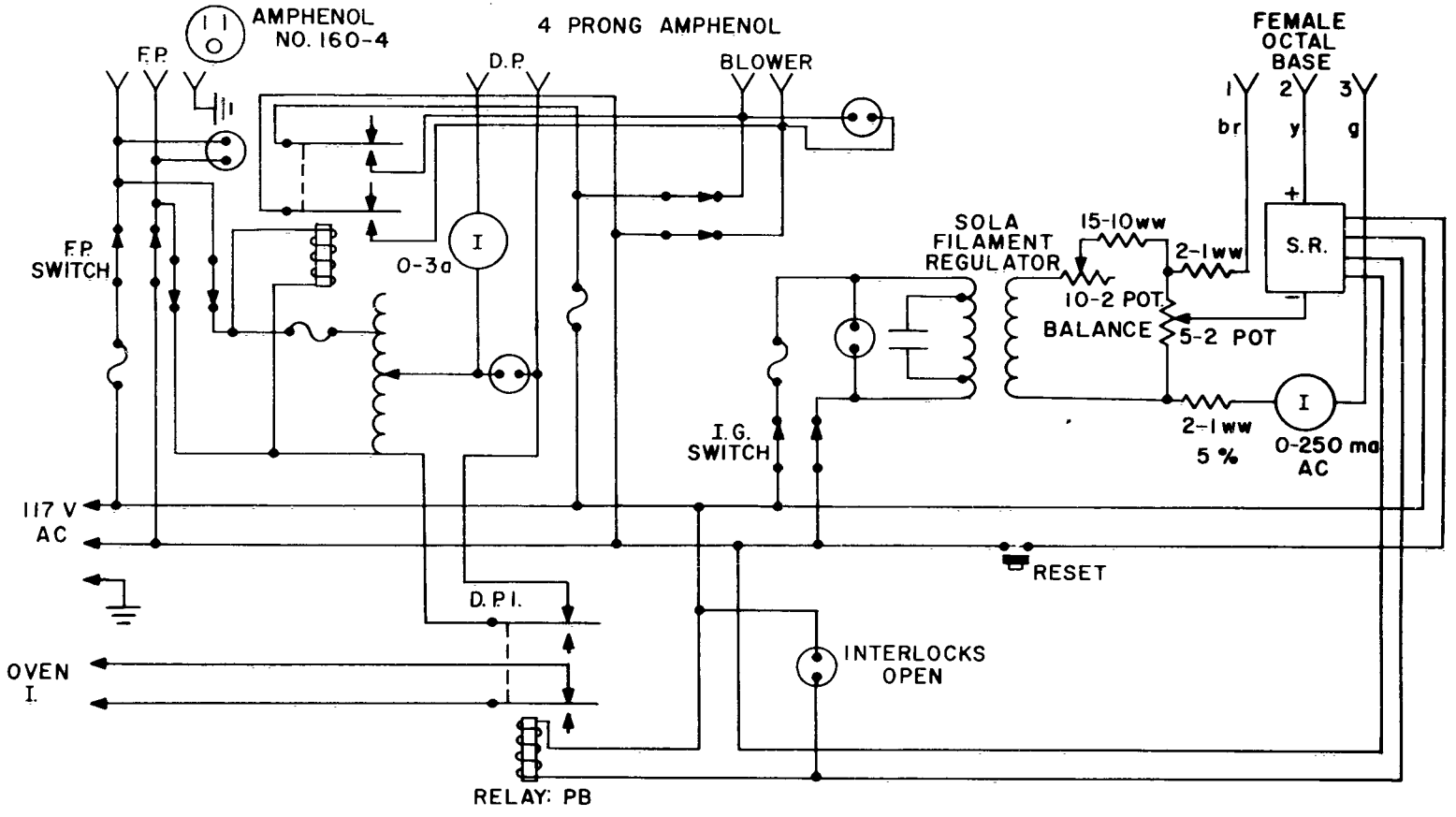

FIG. 4.11 MAIN CONTROL PANEL CIRCUIT

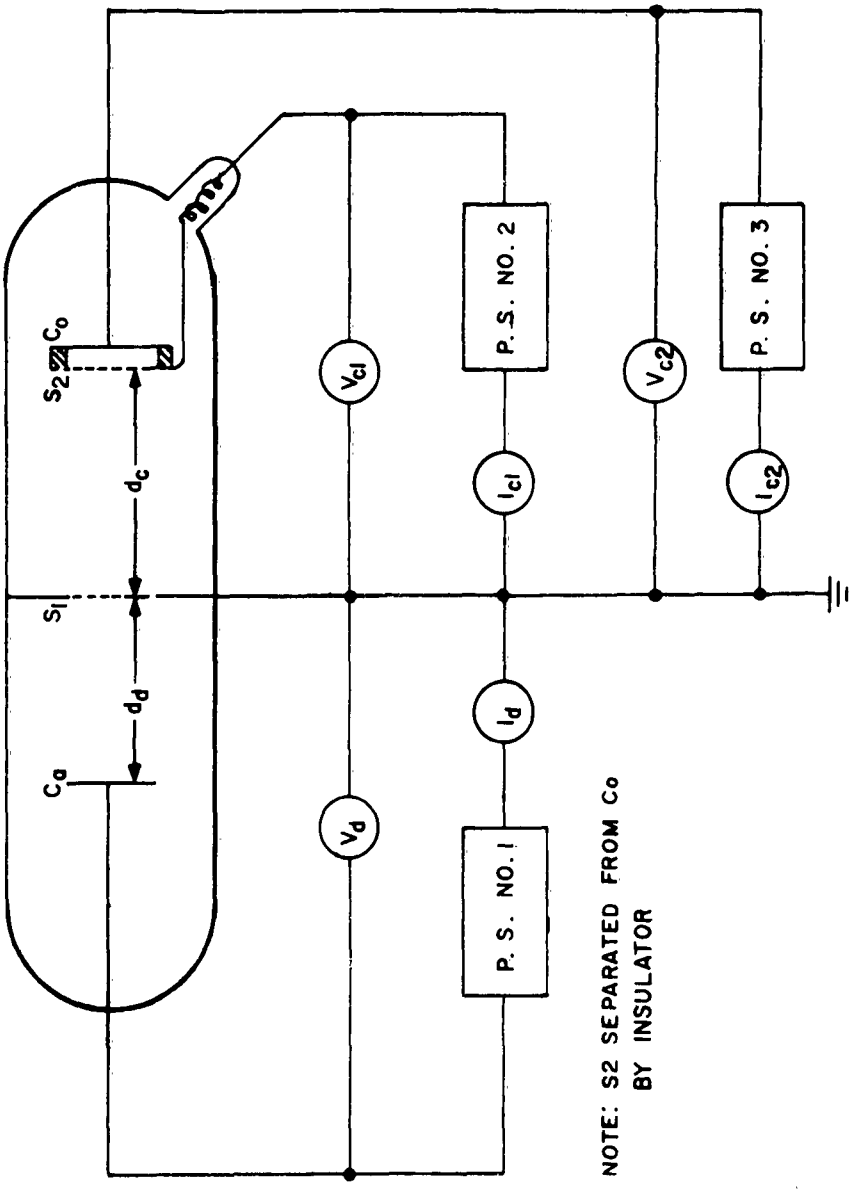

NOTE: S2 SEPARATED FROM Co BY INSULATOR

FIG. 4.12 MEASURING CIRCUIT

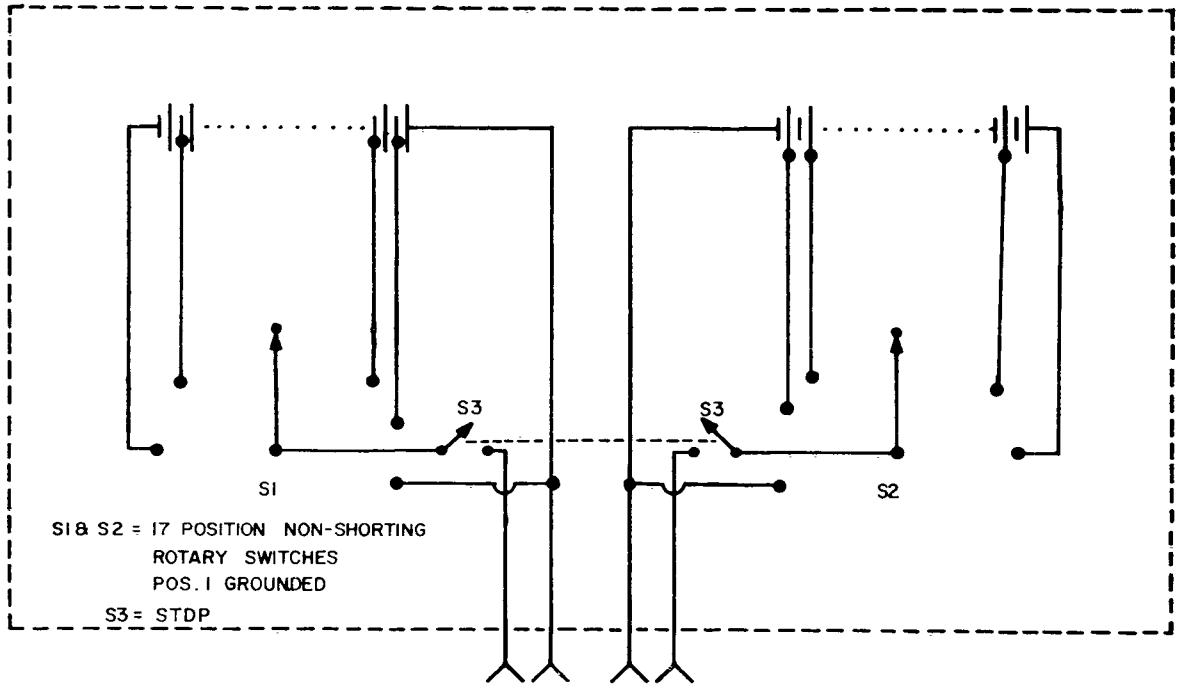

FIG. 4.13 COLLECTOR VOLTAGE SUPPLY

TABLE 4.1

ELECTRONIC EQUIPMENT

Instrument	Manufacturer	Model	Parameter Measured	Range and Accuracy(%)	Serial No.
D. C. Differential Voltmeter	J. D. Fluke Co.	825AR	V_d	(0-500vdc) (±0.01)	(154)
Electrometer Voltmeter	Keithly Instruments	151R	V_{c1}	(0.001-10vdc) (± 1)	(15282)
(One of the above Voltmeters)	. . . . .	. . .	V_{c2}	. . . . .	. . .
Micro-Microammeter	Keithly Instruments	414	I_{c1}	(10μμa-10mA) (± 1)	(19745)
Micro-Microammeter	Keithly Instruments	414	I_{c2}	(10μμa-10mA) (± 1)	(17134)
Meter on PS1 below	Hewlett Packard	712B	I_d	(0-200mA) (± 1)	. . .
Power Supply, PS1	Hewlett Packard	712B	. .	(0-200mA) (± 1) (0-500vdc) (± 1)	(022-04430)
Power Supply, PS2	(Mercury battery)	(See Fig. 4.13)		(0-30vdc)	. . .

temperature the residual gas pressure in the tube is normally 5×10^{-9} mm Hg. The tube is then filled with the gas at the desired pressure and a dc discharge is maintained in the discharge section until the burning voltage of this discharge becomes stable. This insures a thorough cleaning of the cathode by the sputtering process.

References

1. M. A. Biondi, Rev. Sci. Instr. 30, 831 (1959).

2. M. A. Biondi, Rev. Sci. Instr. 24, 989 (1953).

Chapter 5

Measurement of the Properties of the Emitter

5.1 Introduction

When studying the laws governing the behavior of a gas diode a hot cathode is generally used as the charged particl : emitter. This has the disadvantage, especially at close spacing, of the creation of an appreciable temperature gradient and consequently a neutral particle density gradient. In order to avoid the inherent complications in the derivation of the formulae relating to the passage of the charged particles through the gas diode, the emitter used in the present experiment is kept cold. The cold emitter consists of a very fine mesh screen and acts also as the anode of a discharge which is maintained behind the emitter. The properties of the auxiliary discharge obviously determine the properties of the cold emitter. The relationship between these properties was the purpose of the studies to be presented in the next chapters. The two quantities of importance are a) the amount and type of particles leaving the emitter and b) the energy distribution of these particles; as a matter of fact, this distribution determines the "temperature" of the cold-"hot" emitter.

In the next two sections, the variables influencing these quantities will be discussed.

5.2 The Discharge Voltage - Electrode Distance Relation

The properties of the various regions of a dc self-sustaining gaseous discharge are well-known.[1-3] The regions of interest in this discussion are the Faraday dark space and the anode fall.

One of the most important characteristics of a dc discharge is that the potential distribution is almost independent of the cathode-anode spacing for fixed discharge current as long as the anode is situated in one of these regions.

By adjusting the discharge parameters appropriately, therefore, it is not only possible to determine the potential distribution in these two regions but also to place the cold emitter (S1) in any one of them. The type of charged particles passing through the emitter and thus entering the collector region is determined by the potential distribution in the discharge region adjoining the emitter. The number of particles "emitted" depends on the charged particle density in the discharge region adjacent to the emitter.

The remaining part of this section will be devoted to a discussion of the voltage-spacing relation and other properties of the two discharge regions of interest.

In the Faraday dark space, ionization and excitation processes are mainly due to (a) the absorption of resonance radiation from both the negative glow region and positive column and (b) the secondary collision processes. In the major part of this region the ionization and excitation processes by electron-neutral interaction are almost absent. The electric field is zero or very small in comparison with the fields in the other regions of the discharge. Since the field is small, the current in this region consists mainly of the diffusion current of positive ions and electrons. The electron current collected by the anode predominates

because of the smaller mass of the electrons. Therefore, if the Faraday dark space is adjacent to the emitter (S1) both ions and electrons can be expected to pass through the screen due to the extremely small electric field in this region.

Ahsmann[4] has derived an expression for the length of the Faraday dark space when the electric field strength is identically zero in this region, so that the currents are exclusively due to diffusion currents. Assuming a plane parallel geometry and only one type of positive ion present the current equations, for this very special situation, read

$$J_e = - eD_e \frac{dn_e}{dx} \qquad (5.1a)$$

and

$$J_p = eD_p \frac{dn_p}{dx} \quad , \qquad (5.1b)$$

where D, n and e are the diffusion coefficient and the density of the charged particles and the electronic charge respectively. The subscripts e and p refer to electrons and ions, respectively. Since the electric field is assumed to be zero, Poisson's equations require that $n_e = n_p = n$ for all values of the coordinate x. Therefore, also $\frac{dn_e}{dx} = \frac{dn_p}{dx} = dn/dx$. The Eqs. (5.1) can then be solved, by eliminating dn/dx and using the total current $J_t = J_p - J_e$, to give

$$J_p = \frac{D_p}{D_e - D_p} J_t \qquad (5.2)$$

for the ion current expressed in terms of the total current. When this condition is satisfied the electric field is zero in the Faraday dark space.

Substitution of (5.2) in (5.1) gives them for the particle density as a function of x, the relation

$$n(x) = n(o) - \frac{J_t}{e(D_e - D_p)} x \quad , \qquad (5.3)$$

where n(o) is the particle density at the beginning of the Faraday dark space.

Obviously, the maximum value d_1 of x, for which (5.3) can be satisfied is given by

$$d_1 = \frac{en_o(D_e - D_p)}{J_t} \quad . \qquad (5.4)$$

This means that for E = o the length of the Faraday dark space is very close to d_1, since the particle density at the anode is small with respect to n(o).

In contrast to the very small change in potential when traversing the Faraday dark space, the potential increases very fast in the anode fall region.

The sharp rise in potential is due to the fact that the decrease in the particle density gradient in the Faraday dark space

requires that the electric field be increased in order to maintain a constant value of the electron current to the anode.

The total potential difference across the anode fall is equal, in general, to the effective ionization potential V_e of the gas or gas mixture used. For neon the effective ionization potential V_e is equal to its ionization potential, while for a Penning mixture, such as a neon-argon mixture, V_e is equal to the metastable excitation potential of the parent gas (16.6 electron volts for a neon-argon mixture).

It is possible to derive an equation for the thickness of the anode fall in two limiting cases, i.e., the states in which no collisions and many collisions of the electrons occur inside the anode fall region.

The first formula, relating to the "vacuum" case, follows immediately from Eq. (2.10), which was derived for the vacuum diode. It is realistic to approximate the electric field at the beginning of the anode fall region by E = 0. Equation (2.10) then gives

$$d_2 = \frac{2}{3}\left[\epsilon\left(\frac{2e}{m}\right)^{1/2}\right]^{1/2}\frac{V_e^{3/4}}{J^{1/2}} \quad . \qquad (5.5)$$

When many particle collisions occur, the assumption which might be applicable is that for the electron drift velocity the mobility relation holds throughout the entire anode fall region. The following relation for d_2 can then be easily obtained from Eq. (2.24):

$$d_2 = \left[\frac{eK}{(n+1)p_o^n} \left(\frac{n+2}{n+1} \right)^{n+1} \frac{V_e^{n+1}}{J} \right]^{\frac{1}{n+2}} \qquad (5.6)$$

It is believed that the formula (5.5) is a better approximation than (5.6) since the anode fall region is generally very thin. The potential distribution inside this region should follow, for the two limiting cases discussed, the functional dependence on x as implied by the relevant equations.

From the properties of these two discharge regions discussed, the following conclusions can be drawn:

(a) When the screen anode is placed in the Faraday dark space, it is possible for both electrons and ions to be injected into the collector region.

(b) When the emitter is placed in the anode fall region, only electrons will be injected into the collector region. The ions have an average energy close to that of the gas atoms and a small retarding voltage, therefore, is sufficient to repel the ions from the screen anode.

5.3 Energy Distribution of the Emitted Particles

Electrons and ions in the Faraday dark space are generally assumed to have a Maxwellian distribution. The observation and discussion of departures from a Maxwellian distribution have been reported in the literature.[5-9] When the emitter is located in the anode fall the energy distribution of the electrons entering the collector region will consist of a Maxwellian distribution f(v) superimposed on a drift velocity v_o which, when neglecting

collisions inside the anode fall region, corresponds to the change in potential that the electrons experience in passing through this region.

5.4 Measuring Method

The dependence of the discharge maintenance voltage V_d on the cathode-screen anode spacing d_d (Fig. 4.12) is measured for constant discharge current I_d. The data are presented in the next chapter.

Referring to Fig. 4.12, the velocity distribution of the electrons passing through the screen anode into the collector region is determined, for constant discharge parameters, by placing the collector assembly (S_2 and C_0) very close to the screen-emitter (S1). Then the total current $Ic_1 + Ic_2$ collected by the collector assembly is measured as a function of the retarding voltage Ve_1, under the condition that $Ve_1 = Ve_2$. After these preliminary measurements the voltage Ve_1 between (S1) and the screen (S2) is adjusted to an appropriate value. By measuring Ic_2 as a function of Ve_2 the velocity distribution of the electrons crossing the potential barrier Ve_1 is analyzed in more detail.

References

1. F. M. Penning, "Electrical Discharges in Gases," The Macmillan Co., New York, 1957 (42).
2. A. von Engel, "Ionized Gases," Oxford University Press, New York, 1955.
3. J. D. Cobine, "Gaseous Conductors," Dover Publications, Inc., New York, 1958 (213).
4. G. J. M. Ahsmann, Proceedings of the Fifth International Conference on Ionization Phenomena in Gases, pp. 306-314, North-Holland Publishing Co. (1961).
5. I. Langmuir and H. Mott-Smith, Gen. Elect. Rev. 449, 538, 616, 762 (1924).
6. K. T. Compton and I. Langmuir, Rev. Mod. Phys. 2, 222 (1930).
7. P. M. Morse, W. P. Allis and E. S. Lamar, Phys. Rev. 48, 412 (1935).
8. J. M. Anderson, General Electric Research Laboratory Report No. 58-R1-2010, August, 1958.
9. D. H. Pringle and W. E. Farvis, Phys. Rev. 96, 536 (1954).

Chapter 6

Results and Discussion

6.1 Introduction

The experimental data concerning the length of the Faraday dark space and the variation of the potential in this region are presented in Sec. 6.2. The results obtained are compared with those of other investigators.

In Sec. 6.3 the thickness of the anode fall region is compared with the value calculated from the formulae of Sec. 5.2 when inserting the appropriate values for the quantities appearing in these formulae. The value of the potential difference across the anode fall region is compared with the expected value.

The measured retarding potential-collector current relationships are given in Sec. 6.4 and the values for the electron "temperature" calculated from these curves are compared with the data obtained by other authors.

The measurements were carried out in helium at gas pressures of 12, 15.5 and 16 Torr. The cathode used for the auxiliary discharge was a planar electrode with diameter 43 mm. The discharge current was 50 milliamperes.

The specifications of the screen in the anode used is as follows:

optical transparency:	85 percent
number of wires per cm:	40
diameter:	9.5 mm
thickness:	0.025 mm

The diameter of the effective anode, including the screen was 50 mm.

6.2 Faraday Dark Space Region

The variation of the potential in the Faraday dark space has been measured under various conditions, and Fig. 6.1 is representative of the results obtained. Sufficient time was allowed between measurements (about five minutes) so that the discharge was in thermal equilibrium during the period of measurement. It can be noted from this figure that the potential attains a minimum about two millimeters away from the negative glow region, and that the field in the remaining part of the Faraday dark space is about -2.4 volts/cm. At the end of the Faraday dark space (d_d = 11 mm in Fig. 6.1) the potential rises abruptly and the anode fall region starts to develop. The measured potential difference of about 2 volts across the Faraday dark space may be due to the influence of the reversed electric field at the anode, which is present as long as the anode is located within the Faraday dark space region.[1] The magnitude of this reversed field changes with location.

From Fig. 6.1 the length of the Faraday dark space (d_1) is found to be approximately eight millimeters. Since d_1 could not be calculated directly from Eq. (5.4) because n_o was not known, Eq. (5.4) was used to determine n_o.

The current density J_t = 41 amperes/m^2, the length d_1 = 8 mm of the Faraday dark space and the diffusion coefficient of electrons

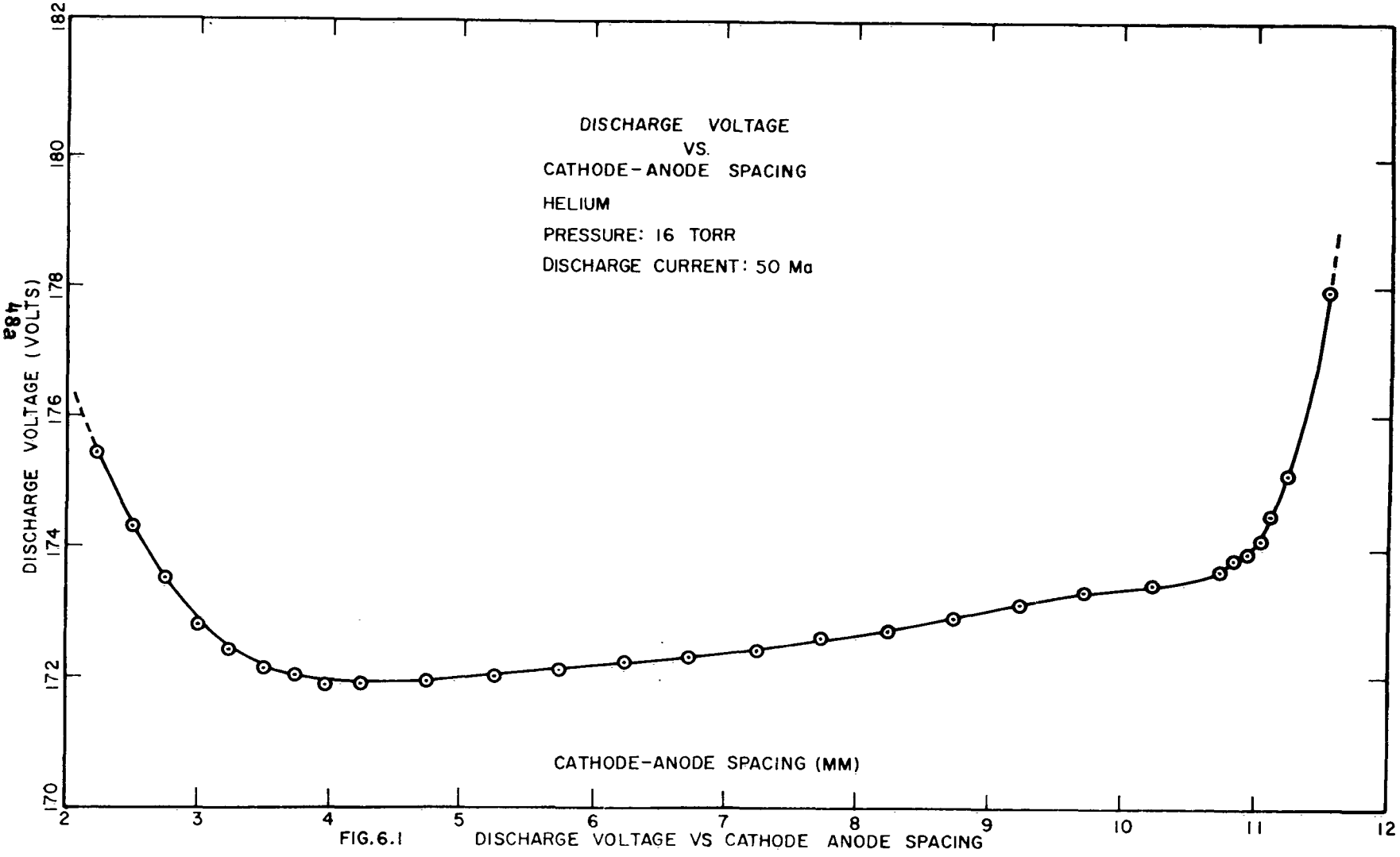

FIG. 6.1 DISCHARGE VOLTAGE VS CATHODE ANODE SPACING

(at 16 mm Hg) D_e = 1.5 m^2/sec, as estimated from Phelp's data for the electron mobility. Using these values the electron density n_o at the beginning of the Faraday dark space is found to be n_o = 1.2 x 10^{16} electrons per m^3, which is a reasonable value for the experimental conditions.

It was found that the data referring to the Faraday dark space are rather sensitive to the surface condition of the two discharge electrodes. Although the general shape of the potential distribution remains conserved, the value of the length as well as the magnitude of the potential differences may change depending on the cleanness of the electrodes. This is in agreement with observations made by Ahsmann.[1]

6.3 Anode Fall Region

The high location accuracy of the screen anode, due to the use of the cathode positioner as described in Sec. 4.2.1, combined with the precise measurement of potential differences, allowed the potential variation in the anode fall region to be determined very accurately. An example of data obtained is shown in Fig. 6.2. It should be noticed that the potential in the Faraday dark space increases slowly until location A is reached. Between locations A and B the potential increases rapidly and monotonically. Between the B and C the potential is very nearly a linear function of d_d, and in this sub-region of the anode fall the field is found to be about -155 volts/cm. At D the potential increases less rapidly since the electrons start to ionize the neutral gas atoms noticeably and thus creates a greater space-charge density. Between

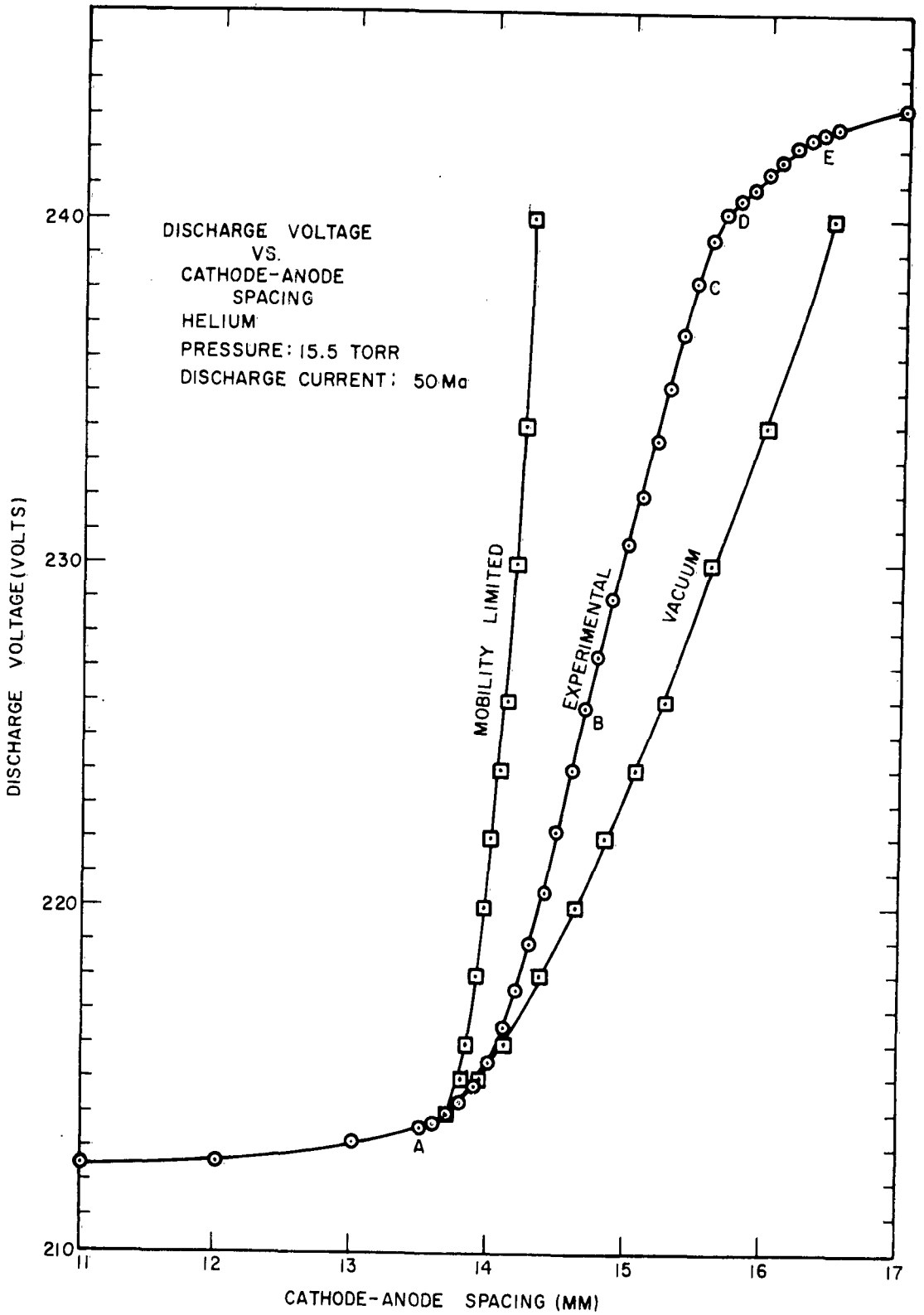

FIG. 6.2 DISCHARGE VOLTAGE VS. CATHODE-ANODE SPACING

points D and E there are two inflection points. This phenomenon is found to repeat itself in the region beyond D and is believed to indicate the beginning of the positive column. Therefore, location D is considered to be the end of the anode fall region. The beginning of this region is more difficult to estimate.

The value of the potential across the anode fall found for five independent measurements under the same operation conditions as in Fig. 6.2 was about 25.4 ± 1 volts, which is in very good agreement with the expected value of about 24.5 volts being the first ionization potential of helium.

The experimental value for the thickness of the anode fall region was determined to be about 1.7 ± 0.3 mm. These values were compared with those obtained from formulae (5.5) and (5.6) which refer to the vacuum diode and gas diode respectively. The measured values of the voltage difference across the anode fall, the tube current density, the gas pressure and the appropriate value for n and K are used in these formulae to make the comparison. The vacuum diode formula gives a calculated value for the thickness of the anode fall region of $d_2 = 2.5$ mm, while the gas diode formula gives $d_2 = 0.6$ mm. The measured value of $d_2 = 1.7$ mm thus lies, as can be expected, between the two values which refer to the two limiting cases of no particle collisions and many collisions, respectively.

The potential distributions inside the anode fall region calculated from the formulae (5.5) and (5.6) are also indicated in Fig. 6.2. The measured curve lies between the theoretical curves, as it should.

6.4 Retarding Potential-Collector Current Relationships

The electron velocity distribution function of the electrons passing through the screen-anode was determined by measuring the current collected by the collector assembly as a function of the retarding potential between this assembly and the screen-anode. Since the screen-anode acts as the emitter for the collector region to be used for the study of the properties of the gas diode, it is essential to know the velocity distribution function of the electrons "emitted" in this way.

In order to reduce the influence of electron-neutral gas particle collisions on the velocity distribution function after being "emitted" by the screen emitter, the collector assembly was placed close to the screen-anode (within 1 mm).

The retarding potential measurements give, aside from information about the properties of the screen-emitter, also information about the velocity distribution function of the electrons present in the plasma region of the discharge adjacent to the screen-anode. As a matter of fact, the screen emitter-collector assembly combination acts as a type of a screened probe.

Referring to Fig. 4.12, the two types of measurements performed were the following:

(a) The determination of the total retarding curve, in which the current collected by the collector assembly as a function of retarding potential, is measured between emitter (S1) and collector (Co) for the situation that the screen (S2) of the collector was connected with the collector (Co) itself.

(b) The determination of the partial retarding curve, in which the current received by the collector (Co) is measured as a function of the retarding potential V_{C2} between this collector and the screen (S2) of the screened collector when a constant potential difference is maintained between the screen (S2) and the emitter (S1). By biasing the collector screen positive with respect to the emitter, it is possible to eliminate the influence on the current of the plasma ions diffusing through the screen anode. When two groups of electrons with appreciably different energies are present in the plasma the slowest group can be separated from the fastest group by biasing the collector screen with respect to the emitter at an appropriate negative potential. In this case, however, the plasma ions entering the collector region contribute to the collector current.

A typical example of the data obtained is shown in Fig. 6.3 on a linear scale. Total and partial voltage retarding curves on a semi-logarithmic scale are presented in Figs. 6.4 - 6.8 for various locations of the screen emitter in the Faraday dark space. It is evident from these figures that the dependence of the collector current on the retarding potential is not exponential over the potential region studied. If the velocity distribution were truly Maxwellian an exponential dependence would exist and the electron temperature could be determined.

There are several possible reasons for the nonexponential character of the retarding curves, i.e., (a) the velocity distribution is non-Maxwellian, (b) the influence of secondary emission

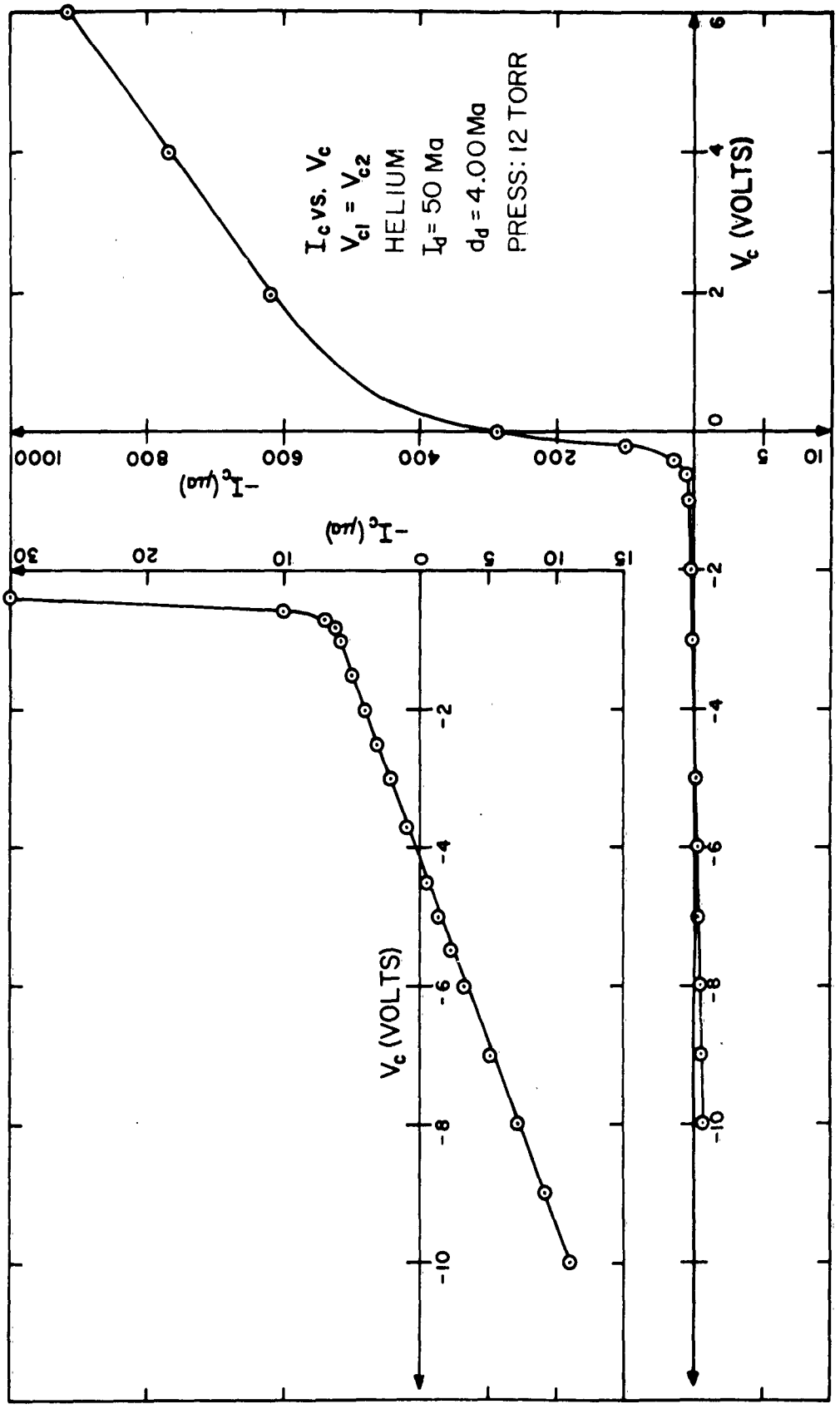

FIG.6.3 TOTAL RETARDING CURVE

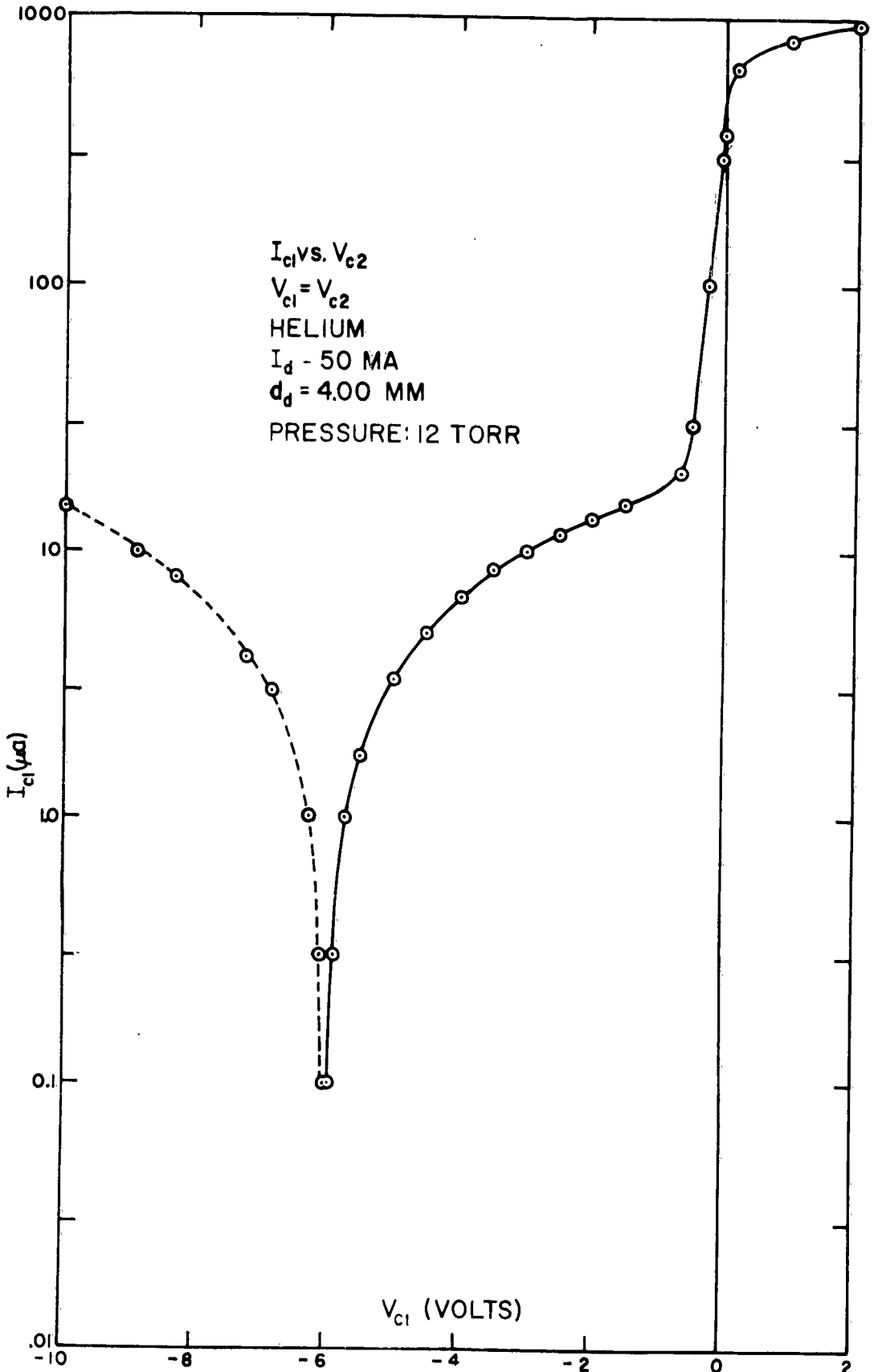

FIG. 6.4 TOTAL RETARDING CURVE

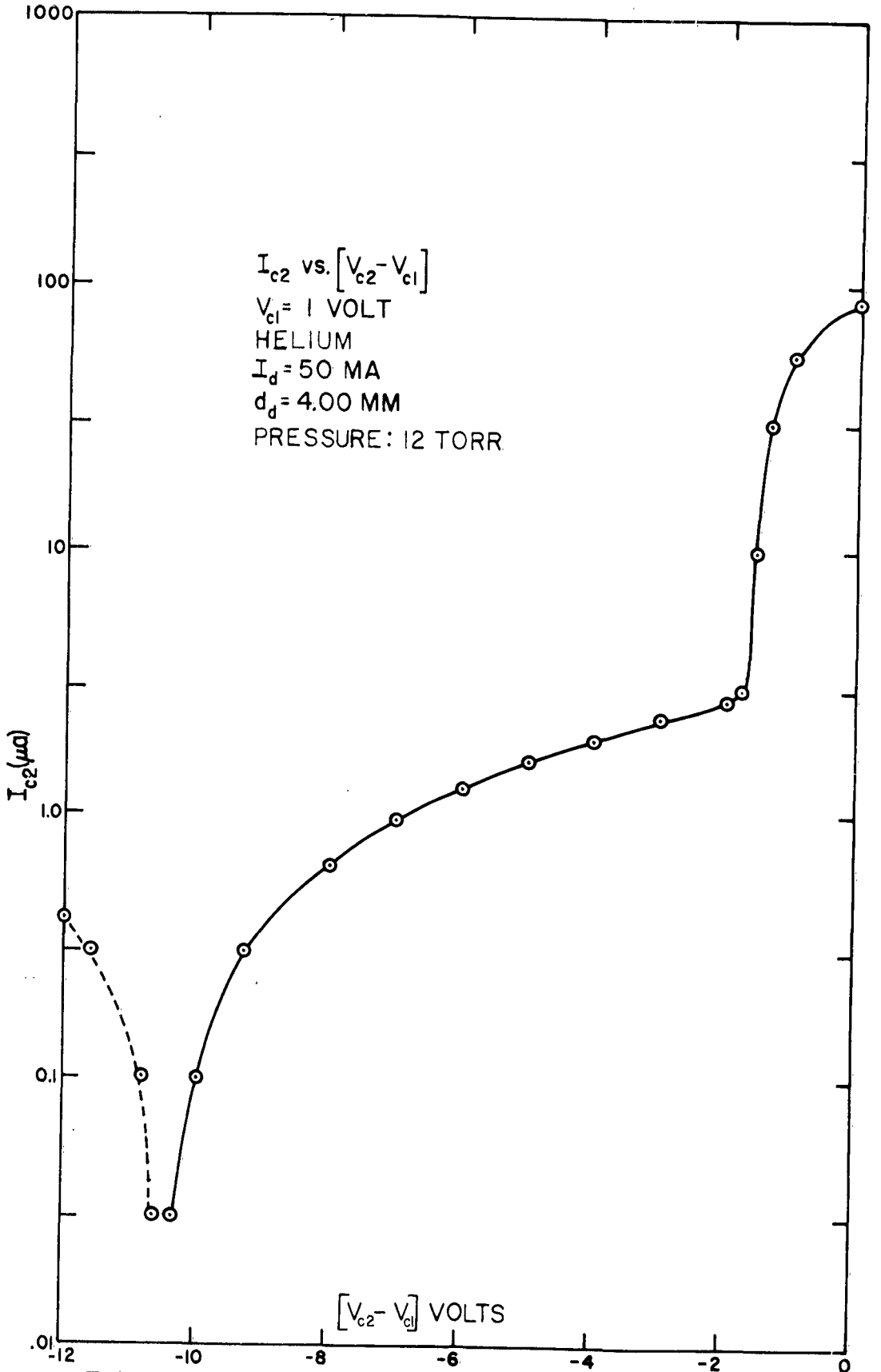

FIG. 6.5 PARTIAL RETARDING CURVE

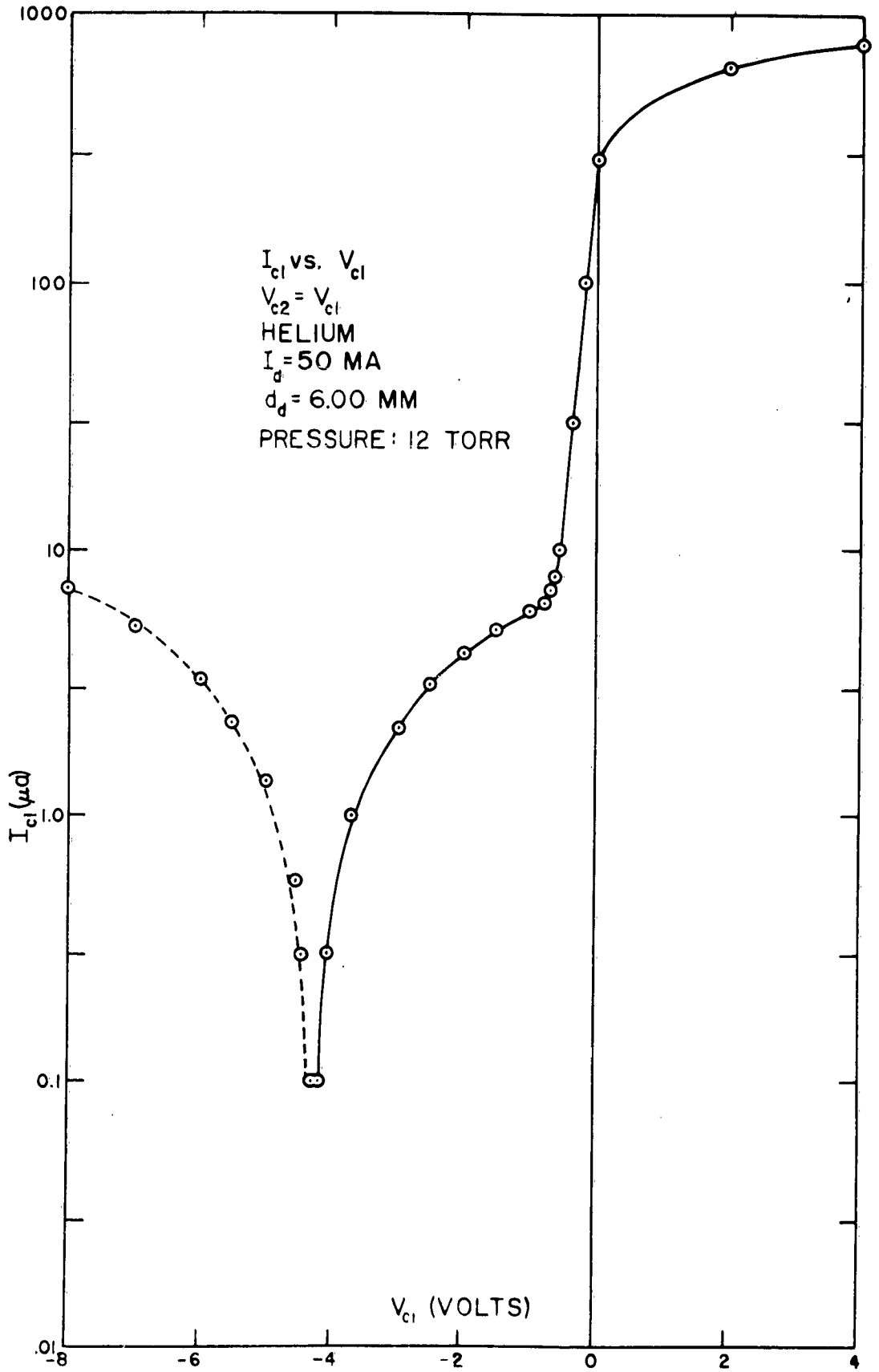

FIG. 6.6 TOTAL RETARDING CURVE

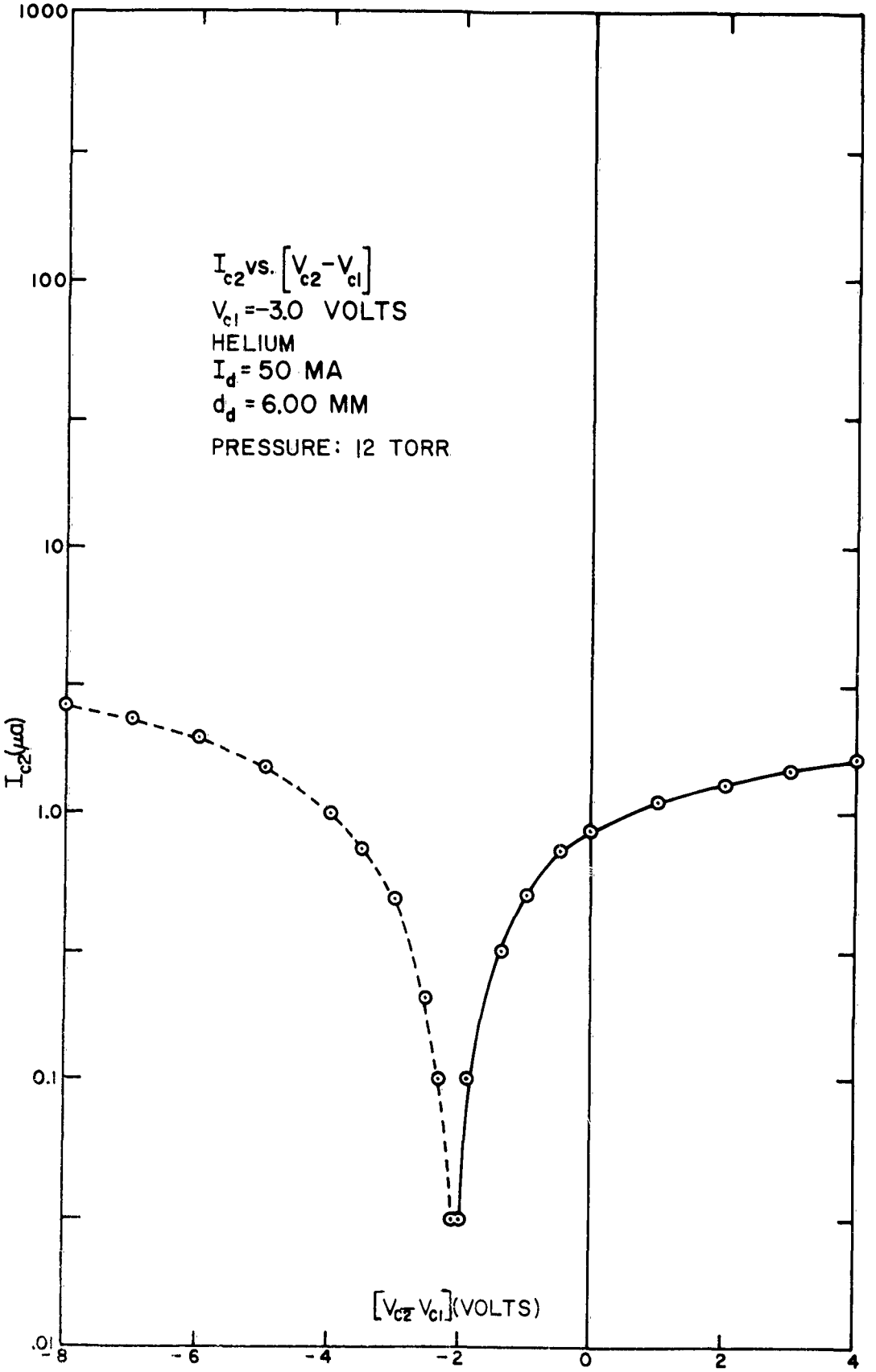

FIG. 6.7 PARTIAL RETARDING CURVE

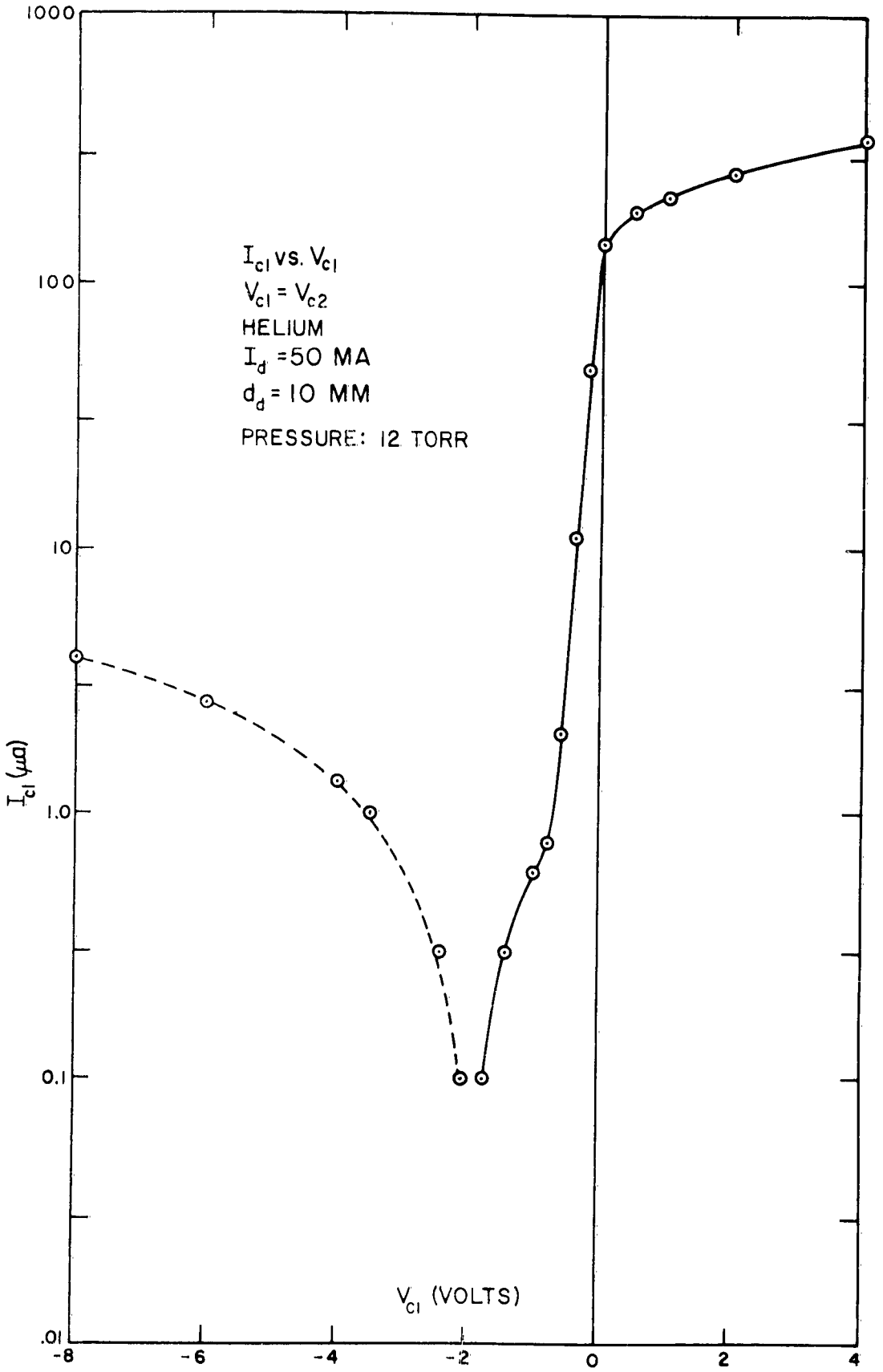

FIG. 6.8 TOTAL RETARDING CURVE

processes may mask the exponential behavior and (c) the electrical transparency of the emitter-screen, as well as of the collector-screen, may be a function of the applied potentials and influence the measurements.

The measurements strongly indicate the presence of two electron groups having widely different energies. This phenomenon has also been observed by other authors,[2-9] and the two groups are called the secondary group (fast group) and ultimate group (slow group). It is observed from Figs. 6.4, 6.6 and 6.8 that the contribution of the group of high-energy electrons to the collected current decreases with increasing distance from the negative glow region.

It is not clear from these measurements that the positive collector current actually saturates at high retarding potentials. Therefore, it was difficult to make the exact corrections necessary to obtain the electron current as a function of the retarding potential. Consequently, the "temperature" of the high energy electron group could only be estimated roughly. The measurement, however, indicated temperatures of about 100,000°Kelvin for this group and, moreover, suggested that the average energy decreases with increasing distance from the negative glow region. This is in agreement with previous studies.[8]

The "temperature" of the slow electron group (ultimate group) could be determined more accurately, since the corrections do not have a large influence here. Values between 1,000 and 2,600°Kelvin were measured depending on the discharge parameters. The

"temperature" of this electron group showed a spatial location dependence analogous to that of the secondary group. These observations are in agreement with those of others.[9]

The reason for the absence of a true saturation of the collector current for large negative potentials and positive potentials, as should occur for the plane probe configuration, is not quite clear. This might be due to (a) the difference between the configuration used in this investigation and an actual plane probe, (b) a dependence of the electrical transparency of the screens on the applied potentials, (c) a multiplication process when high electrical fields are applied inside the collector regions and/or (d) the influence of charged particle reflections at the surfaces of the tube elements.

References

1. G. J. M. Ahsmann, Proceedings of the Fifth Annual Conference on Ionization Phenomena in Gases, pp. 306-314, North-Holland Publishing Co. (1961).
2. K. G. Emeleus and Sloane, Phil. Mag. 14, 355 (1932).
3. Emeleus, Brown and Cowan, Phil. Mag. 17, 146 (1934), where many earlier references are given.
4. Emeleus and Harris, Phil. Mag. 4, 49 (1927).
5. Emeleus, Ballantine, Phys. Rev. 50, 672 (1936).
6. I. Langmuir, Phys. Rev. 26, 585 (1925).
7. D. H. Pringle and W. E. Farvis, Phys. Rev. 96, 536 (1954).
8. J. M. Anderson, General Electric Research Laboratory Report No. 58-R1-2010, August 1958.
9. J. M. Anderson, J. Appl. Phys. 31, 511-515 (1960).

Chapter 7

Summary and Future Plans

The studies reported can be divided into the three following main groups:

(a) The theoretical analysis of the laws governing the space-charge limited current through a gas diode as compared to that through a vacuum diode.

(b) The description of the experimental equipment used during the studies.

(c) The discussion and the measurement of the relation between the parameters of a dc gaseous discharge and the properties of charged particles passing through the screen anode of this discharge.

The theoretical comparison between the properties of the vacuum and the gas diode showed that in the case of space-charge limited current two regions are of interest. The first region (the α-region) is the part of the diode in which the charged particles leaving the emitter are retarded. In the second region (the β-region) the charged particles experience an accelerating field.

The basic laws governing the motion of charged particles in the α-region are quite different for the vacuum and gas diodes. In the vacuum diode the directed velocity of the charged particle is zero as soon as it has traversed a retarding potential difference equal to its directed energy. This makes the analysis of

the α-region when no collisions occur rather simple. However, in the gas diode the randomizing effect of the collisions on the directed particle energy adds to the loss of the directed energy, so that, in general, the particles will have a zero directed velocity closer to the emitter than for the case of no particle collisions. Estimates of the relative importance of the retarding field and the effect of particle collisions are given in Sec. 2.3.3.

The equations to be used in the β-region are the same for the vacuum diode as for the gas diode with the exception that for the gas diode the velocity of the charged particles is determined by their mobility instead of by the traversed potential difference as is the case for the vacuum diode. The formulae for the two types of diodes are compared in Table 2.2 of Sec. 2.3.3.

The relevant formulae are derived by using the monoenergetic method. The validity of this method when, which is generally the situation, the charged particles have a velocity distribution is discussed in Sec. 2.2.4.

The tube to be used for comparing experimental data with the theoretically derived formulae is discussed in Sec. 4.2. In order to avoid a particle density gradient inside the tubes due to the use of a hot emitter which would make comparison with theory complicated and questionable, the emitter used was a fine mesh screen. This screen emitter served as the anode of a cold cathode dc gaseous discharge so that part of the particles arriving at the screen anode pass through this anode and serve as charged particles emitted by the screen cathode. In other words, the

emitter is a cold-"hot" emitter, the "temperature" of which is determined by the parameters of the auxiliary discharge.

The influence of the discharge parameters on the properties of the screen emitter was discussed in Chapter 5. In order to be able to insert in the theoretically derived formulae the proper values for the various quantities, it was found necessary to study carefully the properties of the electrons "leaving" the screen emitter.

One of the important quantities which influences the properties of a diode is the temperature of the emitter, since it determines the number of charged particles emitted as well as their velocity distribution function. Therefore, retarding potential measurements were carried out in order to determine the various electron velocity distributions, thus the range of temperatures, which could be obtained when using the screen emitter. It was found that depending on the parameters of the auxiliary discharge a temperature range of 1,000 to 3,000° Kelvin could be covered. The number of charged particles passing through the screen anode, thus "emitted" by it, depends on the discharge current and the geometry of the screen.

By using a specially developed collector assembly, it was possible to analyze the electron velocity distribution function in detail. Since the electrons passing through the screen anode have properties closely related to that of electrons present in the plasma adjacent to the screen, the variation of the velocity distribution function in the Faraday dark space of a dc discharge

could be determined. This was achieved by placing the screen anode in various parts of this region. Two groups of electrons were detected in a discharge produced in helium. The first group (secondary group) has a large "temperature", while the "temperature" of the second group (ultimate group) was considerably smaller. This is consistent with measurements reported in the literature. The measurements seemed to indicate the conversion of the "hot" group into the "cold" electron group.

By using the screen emitter it is possible to introduce, aside from electrons, also positive ions into the gas diode and thus simulating the surface ionization process. In order to establish the condition under which ions can enter the gas diode, the potential distribution inside the Faraday dark space region and anode fall region was studied by measuring the maintenance potential of the dc auxiliary discharge, for fixed discharge current, as a function of cathode-anode spacing. These measurements give also information about the development of the anode fall and the results are compared in Sec. 6.3 with theoretical expectations as discussed in Sec. 5.2.

Summarizing, the studies reported in the preceding chapters resulted in

(a) a theoretical comparison of the properties of the gas diode with those of the vacuum diode,

(b) the development and construction of equipment needed for the comparison of theoretically derived formulae with experimental data,

(c) a new technique for measuring the variation of the velocity distribution function of electrons in the Faraday dark space of a dc discharge,

(d) the construction of a cold-"hot" cathode, the properties of which can be varied rather easily and

(e) the possibility to study the properties of a gas diode with and without the presence of the surface ionization process.

The studies planned for the future are the following:

(a) By using the flexibility of the cold-"hot" cathode the theoretical formulae presented in Sec. 2.3 for the space-charge limited current of a gas diode will be checked against experimental data.

(b) The influence of the effect of the surface ionization process on the space-charge limited current will be studied.

(c) Measurements of the relaxation time and distance of the velocity distribution function of electrons when a sudden change in the value of the ratio of the electric field and the gas pressure occurs.

(d) Determination of the operating parameters required for initiation of a discharge in the gas diode when the number of electrons leaving the emitter is large with respect to those produced there by secondary production processes.

(e) The study of the efficiency of a discharge as a function of emitter-collector spacing, type of gas and gas pressure, when the discharge is maintained as mentioned under (d).

Air Force Cambridge Research Laboratories, Office of Aerospace Research, Laurence G. Hanscom Field, Bedford, Massachusetts.
Rpt Nr AFCRL-62-438, PROPERTIES OF VACUUM AND GAS DIODES, Scientific Report No. 1, March 1963, 60 pp. illus., 49 refs.

Unclassified Report

Report gives calculations connected with properties of vacuum and gas diodes. Experiments relate to velocity distribution of electrons passing through perforated anode, which serves as electron emitter of

(over)

Unclassified

1. Plasma
2. Vacuum Diode
3. Gas Diode
4. Velocity Distribution
5. Anode Fall

I. Project Task

II. Contract AF19(604)-8072

III. Plasma Physics Research Laboratory, University of Minnesota, Institute of Technology

gas diode. The characteristics of Faraday dark space region and anode fall region of a dc discharge are described and explained.

IV. Prepared by H. J. Oskam and C. B. Johnson